We are IntechOpen, the world's leading publisher of Open Access books
Built by scientists, for scientists

6,100
Open access books available

149,000
International authors and editors

185M
Downloads

Our authors are among the

154
Countries delivered to

TOP 1%
most cited scientists

12.2%
Contributors from top 500 universities

CLARIVATE ANALYTICS
BOOK CITATION INDEX
INDEXED

WEB OF SCIENCE™

Selection of our books indexed in the Book Citation Index
in Web of Science™ Core Collection (BKCI)

Interested in publishing with us?
Contact book.department@intechopen.com

Device, Electronic, Technology for a M.E.M.S. Which Allow the Extraction of Vacuum Energy Conform to Emmy Noether Theorem

Patrick Sangouard

Abstract

This theoretical work corresponds to the hope of extracting, without contradicting EMMY NOETHER's theorem, an energy present throughout the universe: that of the spatial quantum vacuum! This article shows that it should be theoretically possible to maintain a continuous periodic vibration of a piezoelectric structure, which generates current peaks during a fraction of the vibration period. Electronics without any power supply then transform these alternating current signals into a usable direct voltage. To manufacture these different structures, we also present an original microtechnology for producing the regulation and transformation electronics, as well as that necessary for controlling the very weak interfaces between the Casimir electrodes and that of the return electrodes! These vibrations are obtained by controlling automatically and at appropriate instants the action of the attractive Casimir force by a repulsive Coulomb force applied to return electrodes. The Casimir force appearing between the two electrodes of a reflector deforms a piezoelectric bridge, inducing a displacement of the barycenter of the ionic electric charges of the bridge. This internal piezoelectric field attracts opposing moving charges, from the mass, on either side of the piezoelectric bridge used by the Coulomb force used to generate an opposing Coulomb force.

Keywords: Casimir, coulomb, vacuum quantum energy extraction, piezoelectric, MEMS, NEMS

1. Introduction

1.1 Obtaining an electric current from vacuum?

We know that the quantum vacuum, the energy vacuum, the absolutely nothing, does not exist!
This statement has been proven multiple times and noted in particular by:

- Lamb's shift (1947) of atomic emission frequencies.

- By the force of Van der Waals which plays a very important physicochemical role and had an interpretation quantum 1930 [London] when two atoms are coupled to the same fluctuations in vacuum.

- By Hawking's radiation theory, predicted in 1974 and observed on September 7, 2016.

- By the experimental verification (1958) of the existence of a force equated by Casimir in 1948. This so-called Casimir force was measured for the first time in 1997.

1.2 Brief presentation of Casimir's force

The vacuum energy is the zero-point energy of all fields (tensorial and scalar) in space, which for the standard model includes the electromagnetic field, gauge fields, fermionic fields, as well than the Higgs field. In quantum field theory, this vacuum energy defined as zero, is the ground state of fields! In cosmology, vacuum energy is a possible explanation for Einstein's cosmological constant. It has been observed and shown theoretically that this so-called zero-point energy, is non-zero for a simple quantum harmonic oscillator, since its minimum energy is equal to E = h ν/2 with ν the natural frequency of the oscillator, and h the Planck's constant.

Originally [1], the Casimir effect is derived from statistical fluctuations in total vacuum energy and is the attraction (in general) between two plates separated by a vacuum. In this approach, this Casimir energy is the part E_{CA} of the vacuum energy which is a function of the z_S separation of the Casimir plates, with:

$$E_{CA} = S \left(\frac{\pi^2 \hbar c}{740 z_S^3} \right)$$

This Casimir energy is proportional to the reduced Planck constant h, to the speed of light c and to the surface S of the reflectors (in the limit where the edge effects of the plates are negligible, which then imposes large dimensions of the reflectors compared to that of the separation of the plates).

The force of Casimir F_{CA} between the two reflectors is then the derivative compared to z_s of this energy thus: This Casimir force,

$$F_{CA} = \frac{d(E_{CA})}{dz} = S \left(\frac{\pi^2 \hbar c}{240 z_S^4} \right) \tag{1}$$

proportional to the surface, defines a pressure F_{CA}/S which depends only on the distance z_s^4 between the reflecting plates. This local approach greatly facilitates the formulations of Casimir's forces [1, 2]. The force of Casimir is then attractive and can be understood like a local pressure namely, the so-called virtual radiation pressure and exerted by vacuum fluctuations on the mirrors. These homogeneous, isotropic, and constant fluctuations of the vacuum, manifested by radiation and virtual particles, are modified by the presence of reflecting mirrors. These particles, however real, are called virtual because their lifetimes are noticeably short (for an electron of the order of 6.10^{-22} seconds) before recombining to return to a vacuum!

The presence of the reflective plates excludes wavelengths longer than the distance z_s between the plates. They thus induce a pressure difference of the virtual

particles generated by the vacuum between the internal and external space of the 2 plates. This difference results in a force that pushes the plates together.

The Casimir force between two perfectly conductive and smooth plates, without conductive charge, at zero temperature is written as the difference of the radiation pressures calculated outside and inside the cavity and is then written (**Figure 1**):

$$F_{ca} = S\left(\frac{\pi^2 \hbar c}{240\ z_S^4}\right)$$

The famous physicist Evgueni Mikhaïlovitch Lifchits gave a general formula, which supplements that of Casimir because it considers the effect of temperature [3]. Indeed, when the temperature is no longer zero, the radiation of the black body must then be considered and the Casimir force at temperature T then becomes that of Lifchits [4].

$$F_{ca} = S\left(\frac{\pi^2 \hbar c}{240\ z_S^4} + \frac{\pi^2}{45}\frac{(kT)^4}{(\hbar c)^3} - \frac{kT\pi}{z_S^3}\exp\left(-\frac{\pi \hbar c}{kT z_S}\right)\right) \quad (2)$$

With k the Boltzmann constant and T the temperature. This modification is important for large distances, typically $L \geq 3$ mm at ambient temperature.

We will use Eq. (1) to calculate and simulate the structure defined in the following diagram (**Figure 2**) because the intervals between electrodes are much smaller than μm and the effect of temperature is negligible.
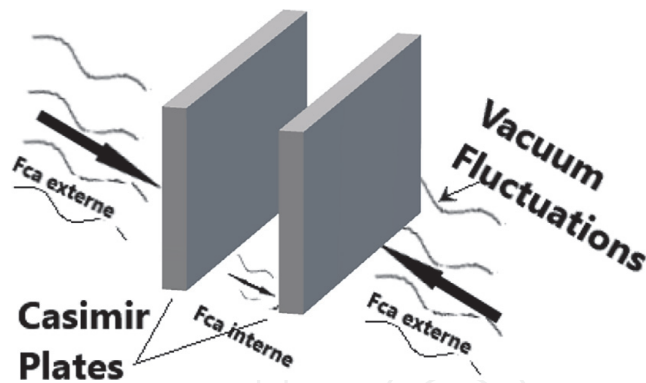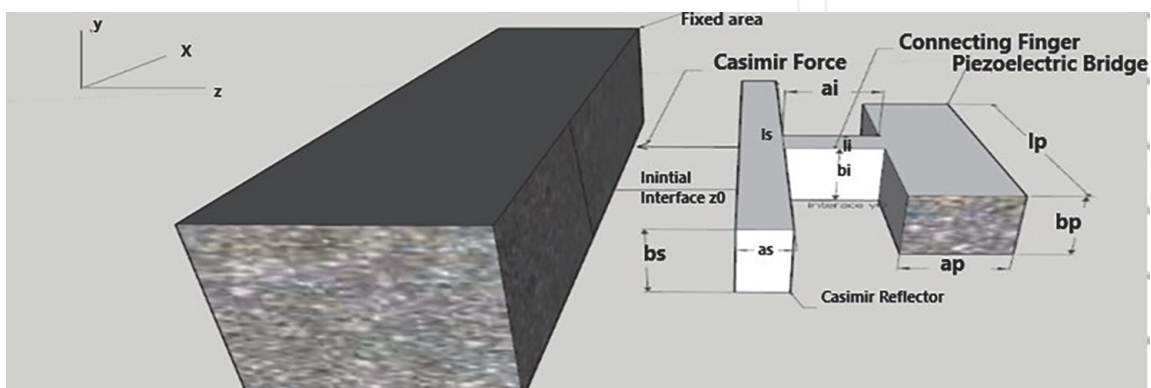

Figure 1.
Casimir effect.

Figure 2.
General representation of the structure.

1.3 Extract energy from the vacuum?

The term *vacuum energy* is sometimes used by some scientists claiming that it is possible to extract energy—that is, mechanical work, heat … ., from the vacuum and dispose thus, ideally, a gigantic and virtually inexhaustible source of energy. Of course, these different hypotheses arouse great skepticism among many scientific researchers because they call into question a principle demonstrated mathematically by the theorem of the mathematician Emmy Noether in 1915, which involves the conservation of energy (like all invariances). This theorem is accepted in physics and has never been faulted until now!

In fact, the problem is less to extract energy from the vacuum than to extract it without spending more energy that we cannot hope to recover! This principle of Noether's theorem, still observed at the macroscopic scale, suggests that extracting energy from a vacuum would require at least as much energy, even probably more, than the process of its recovery would provide.

Thus, a cyclic system, on the model of a piston engine going from a position n°1 to n°2, then from n°2 to n°1, the existence of the Casimir force in $1/zs^4$, therefore greater in position (2) than in (1), would then imply spending more energy to return to (1), which would necessarily require an added energy!! This problem, like that of perpetual motion, then implies that this hope of extracting energy from a vacuum seems impossible and cannot be done with at least zero energy balance! But this is forgetting that an energy is not limited to a force but is, for example, the product of a force (intensity variable) by a displacement (position variable) (see **Figure 3**).

Indeed, imagine that the piston is a piezoelectric bridge, and that the deformation of this bridge is caused by the Casimir force. The deformation of this piezoelectric bridge induces fixed electric charges of opposite sign on each of its faces 1 and 2. Imagine that opposite mobile charge moves from the mass on each side of piezoelectric area. So, if it is possible to propagate, at the right moment, a part of the mobile charges of face 1 for example, on an electrically insulated surface opposite to face 2, then a Coulomb force opposite to the attractive Casimir force would practice. If this Coulomb force is greater than the Casimir force, for example by a factor of at least 2, then the total force $F_t = F_{CA} - F_{CO}$, applied to the center of this piezoelectric bridge deforms it in the other direction, decreases then cancels out its deformation thus the electric charges on the two faces of the piezoelectric bridge. The disappearance of electric charges suppresses the Coulomb force (see **Figures 4** and 5). The system would then return
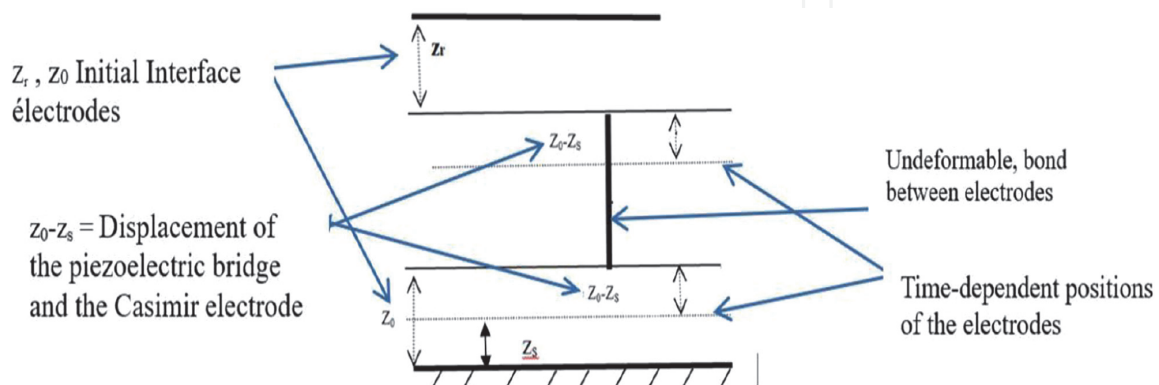

Figure 3.
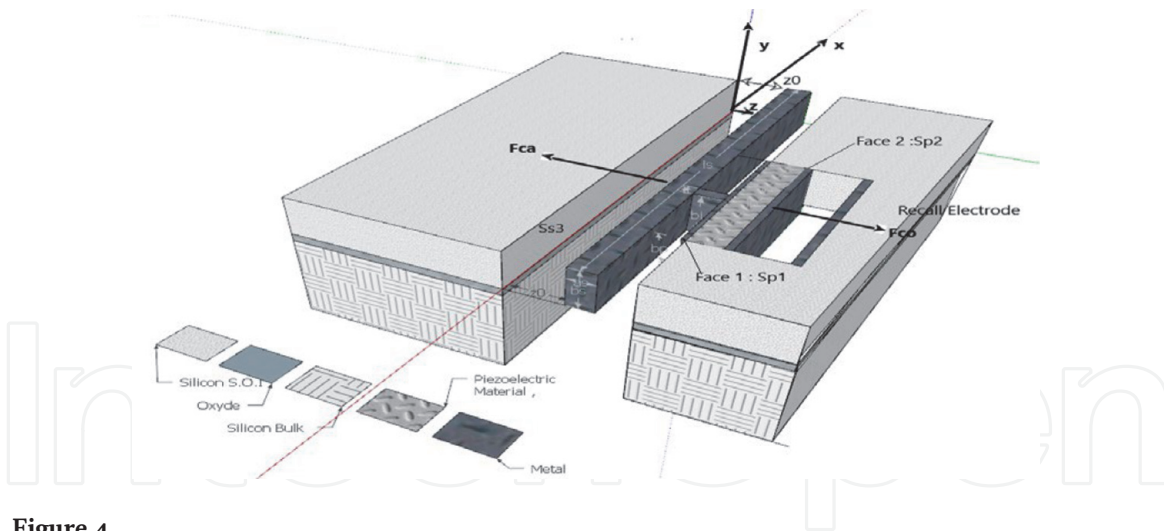*Nomenclature of the different positions for the moving Casimir electrode.*

Figure 4.
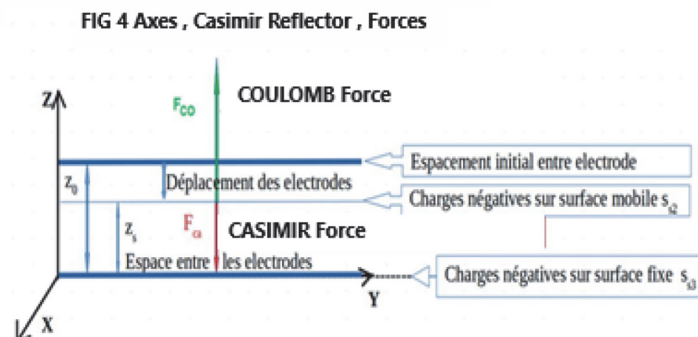*Different view of the device without electronics.*

Figure 5.
Axes, forces, Casimir's electrodes.

to its original position and physical characteristics. Everything would start again, causing vibrations of the piezoelectric bridge of the Casimir reflector device without any external energy input!

Then, on the assumption that all the transient states of the system do not require any input of external energy and are only consequences of a primary cause which is the energy of the vacuum, the principle of Emmy Noether should not be contradicts!

The fixed electric charges on the two metallized faces of the piezoelectric bridge are of opposite signs and attracts from the mass of the mobile charges of opposite signs (**Figure 3**).

Let us imagine that the whole of the return electrode is in two parts of equal areas but separated by a switch circuit consisting of MOSN and MOSP enriched, in parallel and of threshold voltage $Vt_{NE} = -Vt_{PE}$ (**Figure 3**). The first part of this metallic return electrode and surface S_{p1} consists of one of the faces of the piezoelectric bridge and carries mobile electric charges $Q_m = -Q_F$.

The second part of this metal electrode is earthed via another switch circuit made up of depleted MOSN and MOSP, in series and of the same threshold voltage as the enriched MOSN and MOSP: $Vt_{ND} = Vt_{PE} > 0$ and $Vt_{PD} = Vt_{NE} < 0$ (see **Figure 3**).

These switch circuits (circuit 1 = MOSN and MOSP enriched in parallel, circuit 2 = MOSND and MOSPD in depletion and in series), are designed so that they open and close in opposition.

When circuit 1 opens or closes, at the same time switch circuit 2 closes or opens, thus isolating this return electrode from the ground (see **Figure 3**). This opposite behavior of the switch circuits can be seen in **Figure 3**.

So, when circuit 1 is open, the two parts of the return electrodes are grounded through circuits 2, on the other hand when circuit 1 closes the two parts of the return electrodes are isolated!

The electric field inside a perfect conductor being zero, the mobile charges attracted to the first part of the return electrode are redistributed on the two parts of this electrode in the ratio of the homogenization surfaces, that is to say ½ and are opposite the other electric charge face n°2 of the bridge! One then develops, between these isolated electrodes an attractive Coulomb force which is in the opposite direction to the Casimir force and can be greater than it (see **Figures 3–5**).

Now, we know that in the case of a deformation perpendicular to the polarization of a piezoelectric layer and caused by an F_{CA} force, the fixed charges Q_F induced by the deformation of this piezoelectric layer are proportional to the Casimir force F_{CA} and are therefore in $1/z_s^4$, with [5, 6].

$$Q_F = (d_{31}.F_{CA}.l_P)/a_p, \tag{3}$$

With d_{31} = piezoelectric coefficient (CN^{-1}), l_p, a_p respectively length and thickness (m) of the piezoelectric bridge (**Figure 5**). These fixed electric charges on the two metallized faces of the piezoelectric bridge have opposite signs and attract mobile charges of opposite signs from the mass (**Figure 5**). Thus, when it is effective, the Coulomb return force F_{CO} is in $1/z_s^{10}$ because on the one hand in $(Q_F/2)^2$ (therefore in $1/zs^8$) but also in $1/(z_r + z_0 - z_s)^2$ because depending of the distances $z_r + z_0 - z_s$ between return electrode n°1 and face n°2 of the piezoelectric bridge. With z_r the initial distance between the opposite face of the piezoelectric bridge and the return electrode, zs = distance between Casimir electrodes, time dependent, and z_0 = initial distance between Casimir electrodes (see **Figures 3–6**) and **Figure 2** bis. We will choose in the following MATLAB simulations (unless otherwise specified), the same interface between return electrode z_r as that attributed to the initial interface z_0 between Casimir reflectors. The distances over which the free Casimir electrode moves, correlated with
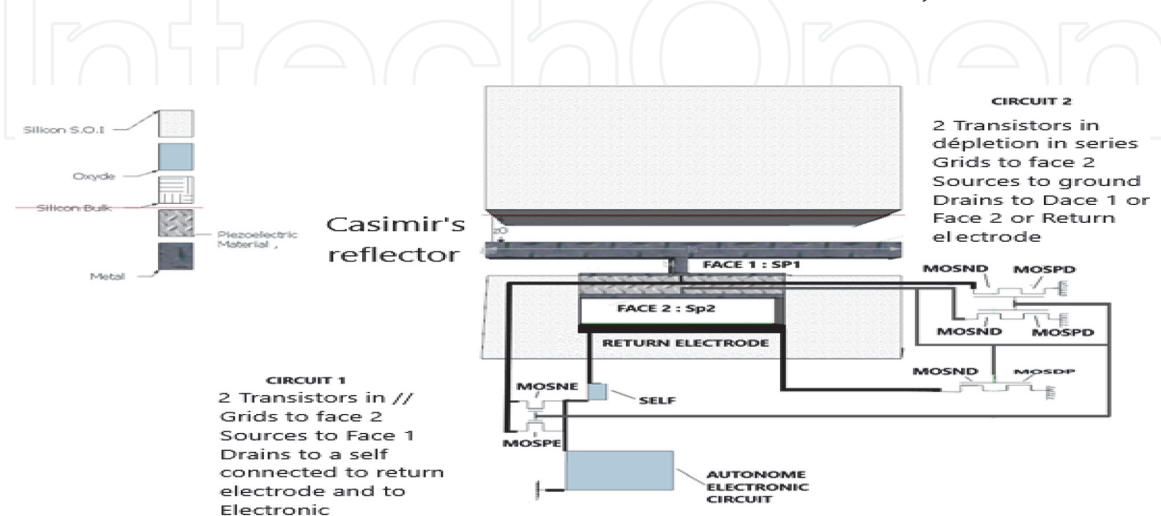

Figure 6.
General configuration of the device: MOS grid connections (face 2 of the piezoelectric bridge: Red), source connections (face 1 of the piezoelectric bridge: Green.

the deformation of the piezoelectric bridge are very small and less than 100 A°. The variations z_0, z_e, z_s are therefore <100 A° and are very small compared to the dimensions of the piezoelectric bridge and that of the Casimir electrodes. Although the rigorous calculation is possible, for the sake of simplification we will first consider that the Coulomb return electrodes remain strictly parallel (**Figures 3–5**).

Considering that the Coulomb force is zero when the piezoelectric bridge has no deformation, we thus obtain an attractive Coulomb force of direction opposite to that of Casimir with:

$$F_{CO} = \frac{Q_F^2}{4\pi\varepsilon_0\varepsilon_r}\left(\left(\frac{1}{z_r + z_0 - z_S}\right)^2\right) =$$

$$\left(S_S \frac{\pi^2\hbar c}{240} \frac{d_{31}l_P}{2^*a_P}\left(\frac{1}{z_s^4} - \frac{1}{z_0^4}\right)\right)^2 \left(\frac{1}{4\pi\varepsilon_0\varepsilon_r}\right)\left(\frac{1}{z_r + z_0 - z_S}\right)^2\right) \tag{4}$$

We note that $F_{CO} = 0$ when the bridge has no deflection (zs = z0), so no electrical charges! With z_r = interface between the face 2 and the return electrode.

This Coulomb Force in $1/z_s^{10}$ can therefore become greater than that of Casimir which is in $1/z_s^4$.

Applied to the piezoelectric bridge, it reduces its deformation, and therefore the induced charges. So, Coulomb's force diminishes and then vanishes when the bridge goes to the starting position n°1 since zs = z0.

For these Coulomb return electrodes generate only a Casimir force that is negligible compared to that of the reflector, it will be necessary to choose interfaces z_r greater than 2z0. For example, if $z_r = 2.z_0$ and the surface of Casimir reflector $S_{s2} = 5^*S_p$ then the Casimir force between the return electrodes will be about 100 times weaker than that linked to the reflector, which is negligible (**Figure 3**).

On the other hand, as F_{CO} depends on the charge accumulated on the piezoelectric bridge in $(1/zs)^8$, the electric voltage that the MOS switches will have to withstand, before being triggered increases with the interface z_r, since the position where $F_{CO} = F_{CA}$ decreases with z_r (see **Figure 7**).

This leads to an increase in the threshold voltages of the different MOS with the increase interface z_r.

This electrostatic attraction of the piezoelectric bridge is possible because the fixed electric charges generated by the deformation of the piezoelectric bridge attract mobile electric charges Q_m of opposite signs from the mass.

Note that if switch circuit n°1 is open, we have seen that circuit n°2 is closed and connected to ground, so the second part of the return electrode is to ground.
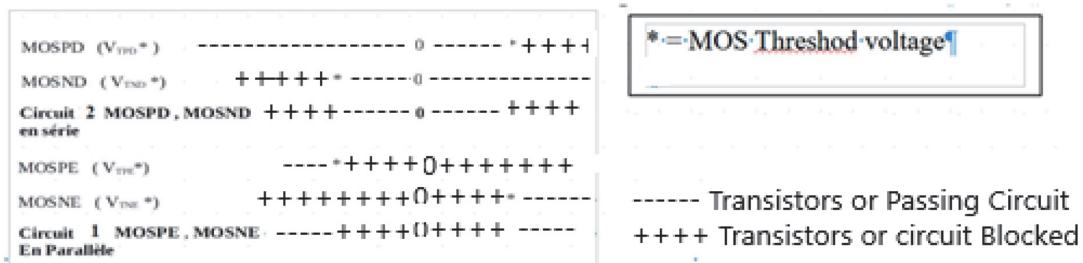

Figure 7.
Distribution of the threshold voltages of enriched and depleted N and P MOS switches.

Conversely, when circuit n°1 is closed then circuit n°2 is open, isolating the second part of the return electrode.

On the other hand, the mobile loads of face 2 by triggering, at the appropriate moment and depending on the threshold voltages, the automatic closing of circuit 1 and the opening of circuit 2, the charges of face 1 are distributed uniformly over the surfaces of the face n°1 of the piezoelectric bridge and the return electrode.

They create an attractive force F_{CO} of Coulomb opposed to that of Casimir which can be superior to him in modulus. The total $F_{CA} - F_{CO}$ force then becomes repulsive and, applied to the piezoelectric bridge decreases and cancels out its deformation, which consequently automatically removes the electric charges on it and initiates the reopening of circuit 1 and the closing of circuit 2.

Thus, the repulsive force of Coulomb disappears, and the force of Casimir becomes preponderant again which allows this cycle to start again!

It seems the spatial and temporal omnipresence of the attractive Casimir force, with the spontaneous appearance and at the appropriate moment of the Coulomb force described above, then generate vibrations of the mobile Casimir reflector plate!

We will calculate the frequency of these vibrations with MATLAB.

Note that during the movement of the piezoelectric bridge from (1) to (2), only the force of Casimir FCA is exerted, because the circuit 2 is conducting and connects the return electrode to the mass suppressing the action of the force Coulomb. Note also that the fixed electrode of the Casimir reflector is constantly earthed (see **Figure 3**).

During the short homogenization time of the mobile charges on the fixed return electrode, an alternating current peak I_a is recovered which generates an alternating voltage peak Ua through its crossing of an integrated inductor (therefore without any additional energy).

This weak and ephemeral but always present electric power $U_a.I_a$ is at the frequency of vibration of the structure. It then activates suitable electronics that must transform—without any external power source—this alternating voltage U_a into a direct voltage U_c which can be used (see Chapter 5).

This electronics was designed when I was working at ESIEE and on abandoned sensors. It works very well in SPICE simulation (see Part V).

If all the components of this project are successful (principle of extracting energy from the vacuum + device generating current peaks at the vibration frequency of the system and converted in peak of voltage by a coil + transformation electronics + technology for realization the device selected), all without any additional energy, the principle of Noether should be validated and the vacuum could then be considered as a simple medium, with which it is possible to exchange energy!

2. Description of the principle used to "extract" energy from the vacuum

As a preamble, we hope and suppose that the events which induce the attractive force of Casimir are exerted in a universal, isotropic, perpetual, and immediate way, if the conditions of separation between reflecting Casimir plates are suitable.

Let therefore be a Casimir reflector device consisting of:

1. a metallized and mobile parallelepiped electrode, of surface $S_{s1} = S_{s2}$ on its 2 lateral faces.

2. a fixed metallized surface S_{s3} separated by a distance z_0 (**Figures 4–6**).

In order for the movement of the movable plate of this Casimir reflector to create electric charges that can be used to induce an attractive Coulomb force, it is necessary that the movement of this movable plate naturally induces a deformation of a structure creating electric charges. A piezoelectric device is therefore required, rigidly connected to the mobile Casimir electrode, so that its induced naturally deformation leads to the appearance of electric charges! And this without any other energy being involved (**Figures 3–5**).

Of course, it is also necessary that the movement of this Casimir reflector mobile plate S_{s2} can be stopped at a chosen and predefined value before the bonding of the surface S_{s2} on the fixed surface S_{s3} takes place! Otherwise, we just definitively collapse the two reflector plates, and no energy extraction is possible! In addition, it is necessary that the mobile system returns to its initial position (or slightly exceeds it).

As said previously, we can then imagine that the attractive Casimir force exerted between the facing surfaces S_{S2} and S_{S3} and which moves the mobile reflector plate S_{S2}, induces a deformation of a parallelepiped piezoelectric bridge of surface S_{P1} and S_{P2}, rigidly linked, by a metal finger, to this reflecting mirror (**Figures 3–5**).

We observe, in **Figure 5**, that the surfaces $S_{p1} = S_{p2} = b_p{}^* l_p$, green or red metallic of the insulating piezoelectric bridge, are connected for:

1. for S_{p1} on the face n°1, through the metal finger (green) to the mobile plate of the Casimir surface reflector $S_{s2} = b_s{}^* l_s = S_{s1}$ which forms one of the electrodes of the Casimir reflector. Thus, the metallic surfaces S_{p1} and the metallic parallelepiped $S_{s1} = S_{s2}$ are equipotential

2. for S_{p2} on the face n°2, at the grids of the switch circuits n°1 and n°2.

The deformations caused by the attractive force of Casimir, then produce fixed electric charges for example $Q_{fn1} = -Q_{fp2}$, on the faces S_{p1} and S_{p2} of the insulating piezoelectric bridge. These fixed charges in turn attract, from the immediate environment (mass or earth) to which they are connected by circuits 2, mobile electric charges Q_{mp1} and Q_{mn2}, respectively. These charges are distributed over the metallized surfaces deposited on the insulating piezoelectric bridge, therefore on S_{p2} and the gates of the transistors of circuits 1 and 2 as well as on S_{p1}, the metal block, the sources of the transistors of circuit 1 and the two coupling capacitors of the electronic transformation circuit (see **Figures 3** and **8**).

Let S_{MOS} be the surface of the gates of the MOS of switch circuits 1 and 2. The mobile charges, for example positive Q_{mp2}, located on the surface S_{p2} of face 2 going to the gate of a MOSNE enriched transistor in the ratio $Q_{mp2MOS} = Q_{mp2}{}^* S_{MOS}/S_{p2}$, then produce a positive voltage $V_G = Q_{mp2\ MOS}/C_{OX}$ on the gate of the MOS transistors, with C_{ox} the gate capacitance of the MOS transistors.

Depending on the sign of these mobile charges on the gates of the MOSNE or MOSPE transistors, they can turn one of them ON, if they are sufficient to induce a voltage V_G greater than their threshold voltage V_{TE}, positive for the MOSNE transistor and negative on the MOSPE transistor in parallel.
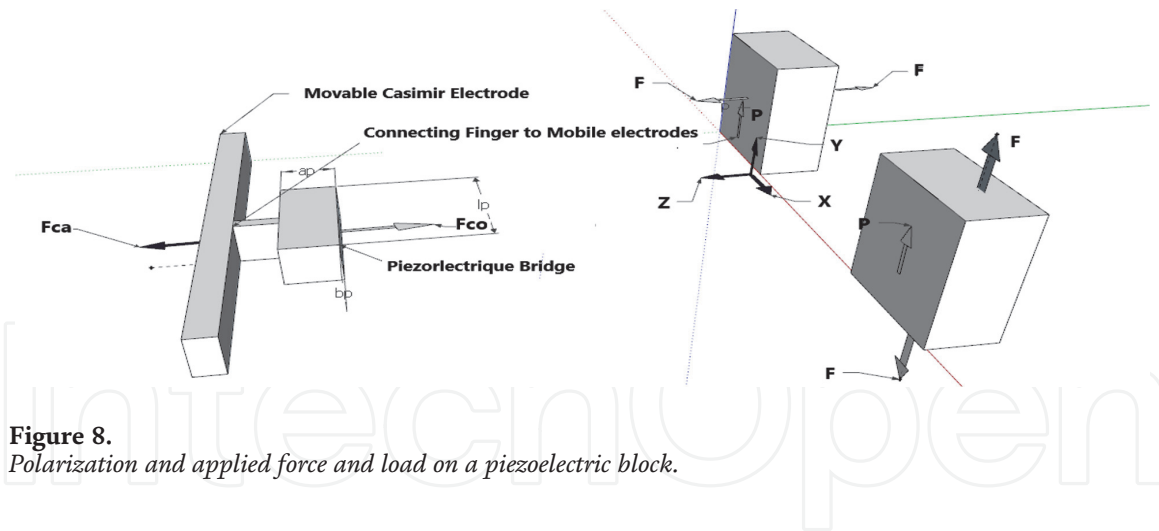
Figure 8.
Polarization and applied force and load on a piezoelectric block.

The nature of these charges depends on the initial polarization of the deposited piezoelectric parallelepiped and on the direction of the deformation imposed by the Casimir force. The sign of these mobile charges on the surfaces Sp1 and Sp2 depending on the real polarization obtained during the realization of the piezoelectric material of this bridge, it is the reverse which occurs if the mobile charges are negative on Sp2, hence the parallel setting of switches! (see **Figure 3**).

As long as this voltage on face 2 of the bridge, for example positive, is less than the threshold voltage V_{TNE} of this MOSNE transistor, the latter remains blocked! Consequently, the mobile charges Qmn1 = −Qmp2 located on the other face Sp1 of the deformed piezoelectric device (connected by a metal block to Ss2) and connected to the sources of the MOSNE and MOSPE remain on these surfaces and do not propagate on the surface of the return electrode. The MOS switches N and P depleted in series from the switch circuit 2 are then on and connect this return electrode to ground (**Figure 3**).

On the other hand, if this voltage V_G becomes greater than the threshold voltage V_{TNE} of the enriched MOSNE, it becomes conducting, and circuit 2 is then blocked, so the mobile charges Q_{mn1}, located on S_{p1} and the metal block can cross the MOSNE to homogenize the charge density on all the return electrodes. These electric charges pass through the inductance L_{IN} in series (**Figure 3**).

When one of the two MOSNE or MOSPE enriched transistors of circuit 1 turns on, then the depleted MOS N and P switches of circuit 2 are blocked. The return electrode, no longer connected to ground, therefore does not discharge these mobile electrical charges and is isolated (**Figure 3**).

Let $S_{p1} = S_{p2} = l_p {}^* b_p$ be the surface area of the faces of the piezoelectric bridge, S_{bloc} = the surface of the metal block of the Casimir reflector (**Figure 5**). Let $S_r = S_{p2} = S_{p1}$ be the surface of the return electrode facing the metallized face S_{p2} of the piezoelectric bridge.

The mobiles charges for example negative $Q_{mn1} = -Q_{mp2}$ which was initially distributed on the metallic surfaces S_{p1} are distributed, after the closing of the MOSNE switch, on the surfaces $S_{p1} + S_r$. They induce between the faces S_{p2} and S_r, electric charges of opposite sign, an attractive force of Coulomb, parallel and opposite to the attractive force of Casimir.

These same electrical charges opposite on the surfaces Sp2 and Sr. become after distribution **as Sp1 = Sr.** This charge Q_{mn1f} remains on the return electrode because circuit 2 is blocked (**Figures 3** and **5**). If the threshold voltages of the transistors are positioned according to $V_{TND} \cong V_{TPE} < 0 < V_{TNE} \cong V_{TPD}$, then we have the following configurations depending on the value of the voltage V_G.

As a result, when circuit 1 is blocked, there is no Coulomb electrostatic attraction between Sp2 and Sr. because the metal return electrode Sr. is grounded and therefore free of charges! However, when circuit 1 is on, circuit 2 is then blocked, so as the metallic return electrode Sr. is isolated, the charges of opposite sign and present on the electrodes S_{p2} and S_r induce an attractive Coulomb electrostatic force!

This attractive Coulomb force as a first approximation is written:

$$F_{CO} = \left(S_S \ \frac{\pi^2 \hbar c}{240} \frac{d_{31} l_P}{2^* a_P} \left(\frac{1}{z_s^4} - \frac{1}{z_0^4} \right) \right)^2 \left(\frac{1}{4\pi\varepsilon_0\varepsilon_r} \right) \left(\frac{1}{z_r + z_0 - z_S} \right)^2 \right) \tag{5}$$

This attractive force triggered by an input of mobile electric charges of opposite sign on the surfaces S_{p2} and S_r is exerted only when the Casimir force between the two reflectors reaches a defined value, dependent on the threshold voltage of the MOSNE transistor.

It will therefore be necessary to adjust the threshold voltage of all these MOSs adequately. Initially, when the piezoelectric beam is not deformed, the electric charges on the faces S_{p1}, S_{p2}, S_{s2} and S_{s3} of the Casimir reflector are zero! The face S_{s2} of the Casimir sole plate, distant from z_0 from the face S_{s3} is then attracted against the fixed face S_{s3}, only by the force of Casimir. This force is communicated via the connecting finger at the center of the face S_{p1} of the piezoelectric bridge and then deforms it.

We will admit in the remainder of this presentation that we are in the case of mode 31 and that, when the piezoelectric bridge undergoes a deformation then the fixed electric charges of the piezoelectric bridge attract negative mobile charges on the electrode Sp1 from the mass and positive mobiles on the other S_{p2} electrode.

If, the threshold voltage of the MOSNE is adjusted so that the Coulomb force is triggered only when $F_{CO} = p \ F_{CA}$ with p proportionality factor 2, then the total repulsion force Ft variable in time and applied to the piezoelectric bridge becomes (**Figures 9** and **10**).
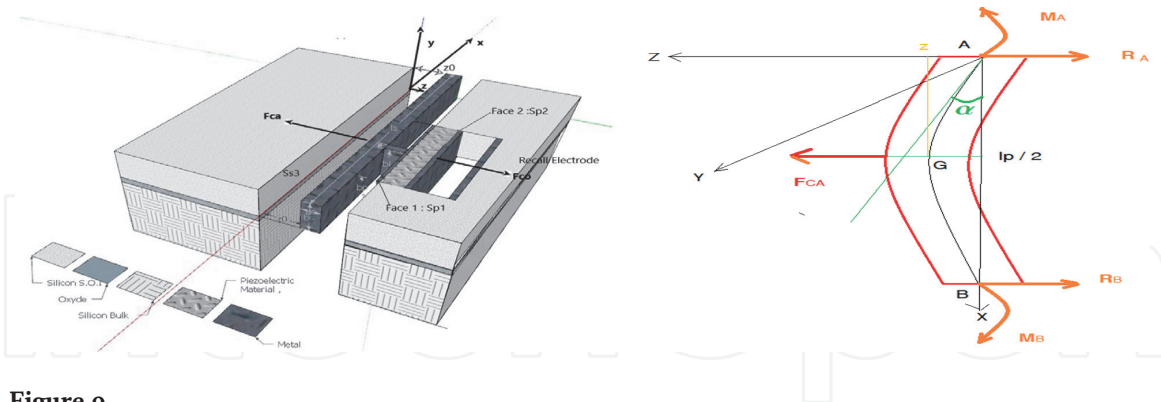

Figure 9.
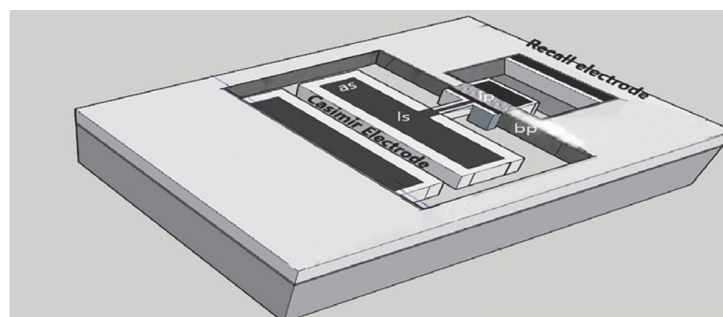*Piezoelectric bridge cutting reactions and bending moment, deflection.*

Figure 10.
Final structure with the metal oxides surrounding the metal electrodes.

$$\overrightarrow{F_T} = \overrightarrow{F_{CA}} - \overrightarrow{F_{CO}} = (1-p)\overrightarrow{F_{CA}} \Rightarrow \overrightarrow{F_T} < 0$$

Becoming repulsive, this force Ft (dependent on time) induces a deformation of the piezoelectric bridge in the other opposite direction, and the piezoelectric bridge returns or slightly exceeds (because of inertia) its neutral position, without initial deformation, therefore towards its position without any electrical charge.

The variation in time of these mobile charges follows, as a first approximation, a law of distribution of the charges on a short-circuited capacitor. Indeed, the fixed electrode S_r initially at zero potential since at ground, is now isolated by switch circuit 2 which is open and isolates it from ground! This temporal variation of the charges is given by the well-known exponential form of discharge of a capacitor according to the formula:

$$Q_{mn} = Q_{mn2} \; Exp\left(-\frac{t}{R_m C_S}\right) \tag{6}$$

This variation in mobile charges stops when these electrical charges Q_{mn} are uniformly distributed over the two electrodes S_{p2} and Sr. and are equal to $Q_{mn2}/2 = -Q_{mn1}/2$ on the two electrodes. Therefore, at time $t_e = R_m C_s \ln(2)$ (Eq. (5)), t_e being the time to reach equilibrium, with R_m the ohmic resistance of the metal track L_{in} of the inductance, C_s the capacitance formed by the electrodes S_{p2} and S_r and the input capacitances of the electronics (**Figure 11**).

This homogenization of electric charges within a metallic conductor:

1. occurs when the gate voltage of the MOSs constituting circuits 1 and 2 exceeds their threshold voltage.

2. induces an attraction of the piezoelectric structure in the direction opposite to that of Casimir.

3. decreases the deformation of the piezoelectric bridge and brings the gate voltage back below the threshold voltage.

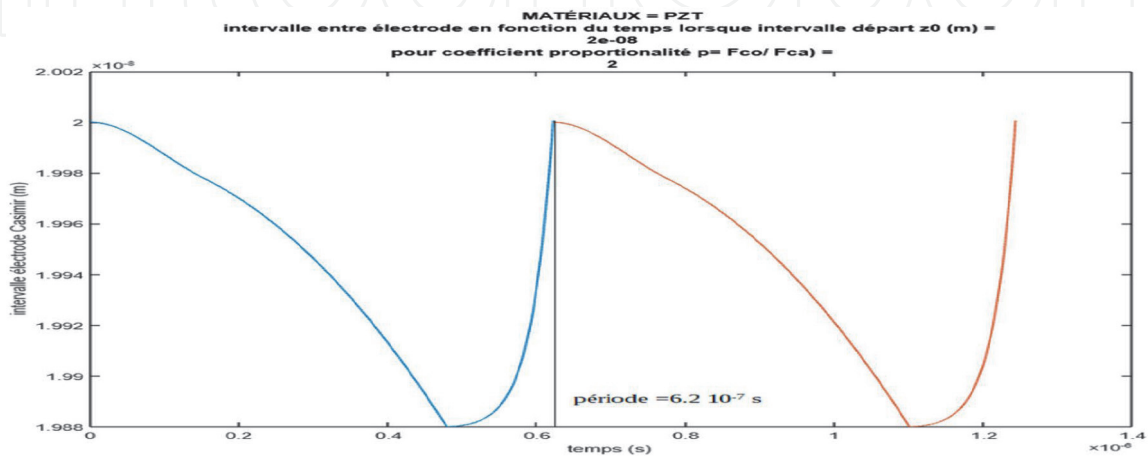4. The transistor MOS only turns off after the charges are homogenized during the short time t_e.

Figure 11.
Interval between casimir electrodes as a function of time for a proportionality coefficient FCO / FCA = 2.

We therefore obtain a current peak during this homogenization with a duration t_e of the order of a nanosecond! This current peak I_{IN} circulating for the duration of time t_e is:

$$IIN = d\frac{Qmn}{d}t'' \quad I_{IN} = -\frac{Q_{mn2}}{R_m C_s}\left(Exp\left(-\frac{t}{R_m C_s}\right)\right) \tag{7}$$

We therefore obtain a current peak during this homogenization with a duration t_e of the order of a nanosecond! A current peak is obtained at time t = 0. With $Q_{mn2}/2$ the charge which is distributed uniformly over the two electrodes S_{p2} and Sr. The time t is counted from the closing of one of the transistors of circuit 1 and the opening of the switches of circuit 2. This current peak I_{IN} crossing an inductance L_{IN} during the time t_e, induces a voltage U_{IN} at the terminals of this inductance L_{IN} as a function of time according to the usual formula:

$$U_{IN} = L_{IN}\frac{d(I_{IN})}{dt} = L_{IN}\frac{Q_{mn2}}{R_m C_s}\left(Exp\left(-\frac{t}{R_m C_s}\right)\right)$$
$$= L_{IN}\frac{Q_{mn2}ln(2)}{R_m C_s t_e}\left(Exp\left(-\frac{t}{R_m C_s}\right)\right) = L_{IN}I_{IN}\ln\frac{2}{t}e \tag{8}$$

There is therefore a voltage peak across the inductance and the electronics appearing without power supply at time t = 0! As the deformations of the piezo-electric bridge cancel each other out during its "rise", the mobile charges on the surfaces S_{p1} as well as S_{p2} also cancel each other out! As a result, the gate voltage on circuit 1 and 2 MOSs drops below the threshold voltages and circuit 1 blocks. Circuit n°2 turns on again and connects face 2 of return electrode to ground, so the electrical charges on the bridge and the Sr. electrode cancel each other out! (see **Figure 5**).

The force of Casimir F_{CA}, still present, again attracts the metallic surface S_{S2} against S_{S3} and the events described above are repeated. Casimir's force deforms this bridge again and it seems that all starts all over again! The consequence is that the structure made up of the piezoelectric bridge, the connecting finger, the metal block forming the mobile Casimir electrode starts to vibrate, with a frequency dependent:

1. Of the Casimir restoring force, and of the Coulomb return electrode Force therefore:

    a. of the starting z_0 and z_r separation interface

    b. geometric dimensions of the different electrodes,

2. Properties of the piezoelectric bridge,

3. The choice of threshold voltages of the different MOS transistors

4. The choice of conductive metal!

As we will see, this frequency is lower than that of the first resonant frequency of the mobile structure if the initial interface z_0 is not weak enough (< 150 A°) to induce a sufficient Casimir force (see Chapters V and X)! An AC voltage peak U_{IN} is therefore automatically recovered at the terminals of the solenoid L_{IN}. This AC voltage peak can then be rectified to a DC voltage of a few volts, by suitable electronics operating without power supply (see amplification electronics without VI power supply).

Before moving on to theoretical calculations and mathematical simulations of the structure we wish to emphasize that the alternating signal U_{IN} is obtained without the input of any external energy!

In conclusions it seems (except errors) that all the electro-physical phenomena leading to a vibration of the structure and to the production of a voltage modulation are only the consequence of a first phenomenon which is at the origin of the Force of Casimir induced by fluctuations in vacuum energy.

They occur naturally and automatically without the input of any external energy except that of a vacuum ... without contradicting Noether's theorem!

3. Calculation of the current generated by the Casimir structure

If the initial separation interface z_0 is greater than 150 A°, the forces present are too weak to induce a vibration frequency of the device corresponding to its first resonant frequency (see Chapter V). We sought the numerical solutions of the differential equations obtained and unfortunately insoluble analytically when the device does not vibrate at its first resonant frequency!

3.1 Calculation of the frequency of vibration of the Casimir structure

Let us calculate the evolution in time of the force of Casimir which is applied between the two electrodes separated by an initial distance z_0. Apply the theorem of angular momentum to this vibrating structure. The angular momentum of the device is

$$\overrightarrow{\sigma^S_{A_{x,y,z}}(structure)} = \overline{\overline{I^S_{A_{x,y,z}}}} \; \overrightarrow{\Omega^S_A} \tag{9}$$

With the angular momentum vector of the structure, the inertia matrix of the structure with respect to the reference (A, x, y, z) and the rotation vector of the piezoelectric bridge with respect to the axis Ay with α the low angle of rotation along the y axis of the piezoelectric bridge.

$$\text{We have because } z << l_p \; sin(\alpha) = \sin(2z/l) \approx \frac{2 \; z}{l_P} \Rightarrow \overrightarrow{\Omega^S_A}$$

$$= \begin{pmatrix} 0 \\ d\alpha/dt \\ 0 \end{pmatrix} \; with \, d\alpha/dt \approx \frac{2 \; dz}{l_P \; dt}$$

Let (Gp, x, y, z), (Gi, x, y, z), (Gs, x, y, z) be the barycentric points respectively of the piezoelectric bridge, of the metal connecting finger and of the metal block constituting the sole mobile of the Casimir reflector. We have (**Figure 5**):

$$\overrightarrow{AG_{P,x,y,z}} = \frac{1}{2}\begin{pmatrix} l_P \\ b_P \\ a_P \end{pmatrix} \quad \overrightarrow{AG_{I,x,y,z}} = \frac{1}{2}\begin{pmatrix} l_P & +l_i \\ b_P & +b_i \\ a_P & +a_i \end{pmatrix} \quad \overrightarrow{AG_{S,x,y,z}} = \frac{1}{2}\begin{pmatrix} l_P & +l_i & +l_s \\ b_P & +b_i & +b_s \\ a_P & +a_i & +a_s \end{pmatrix}.$$

The inertia matrix of the bridge, in the frame of reference (Gp, x, y, z) is

$$\overline{\overline{I^P_{GP}}} = \frac{m_P}{12}\begin{pmatrix} a_P^2 + b_p^2 & 0 & 0 \\ 0 & l_P^2 + b_p^2 & 0 \\ 0 & 0 & l_P^2 + a_p^2 \end{pmatrix} \tag{10}$$

The inertia matrix of the finger is, in the frame of reference (Gi, x, y, z) is:

$$\overline{\overline{I_{GI}^I}} = \frac{m_i}{12} \begin{pmatrix} a_i^2 + b_i^2 & 0 & 0 \\ 0 & l_i^2 + a_i^2 & 0 \\ 0 & 0 & l_i^2 + b_i^2 \end{pmatrix} \tag{11}$$

The inertia matrix of the reflector is, in the frame of reference (G_S, x, y, z) is:

$$\overline{\overline{I_{GS}^C}} = \frac{m_S}{12} \begin{pmatrix} a_S^2 + b_S^2 & 0 & 0 \\ 0 & l_S^2 + a_S^2 & 0 \\ 0 & 0 & l_S^2 + b_S^2 \end{pmatrix} \tag{12}$$

The total inertia of the structure becomes in the reference (A, x, y, z), $I^s_{A,x,y\,z} = I^P_{A,x,y_z} + I^I_{A,x,y,z} + I^c_{A,x,y_z}$ with A at the edge of the embedded piezoelectric bridge and $I^P_{A,x,y,z}, I^I_{A,x,y,z}, I^c_{A,x,y_z}$ is the inertia matrix obtained taking Huygens' theorem applied to this structure. The angular momentum theorem applied to the whole structure gives

$$\rightarrow \frac{d\left(\sigma_{A,x,y,z}^S\right)}{dt} = \overline{\overline{I_{A,x,y,z}^S}} \rightarrow \frac{d\left(\Omega_A^S\right)}{dt} \Rightarrow \overline{\overline{I_{A,x,y,z}^S}} \frac{2}{l_P} \begin{pmatrix} 0 \\ d^2z/dt^2 \\ 0 \end{pmatrix}$$

$$= \overrightarrow{\sum_A Moments\ on\ the\ structure} = \overrightarrow{M_A} + \overrightarrow{M_B} + \overrightarrow{F_{CA}} \wedge \begin{pmatrix} 2/l_P \\ 0 \\ 0 \end{pmatrix}$$

$$with\ \overrightarrow{F_{CA}} = \begin{pmatrix} 0 \\ 0 \\ F_{CA} \end{pmatrix}$$

$$\tag{13}$$

We know (see X), according to the axis of Az that the moments: $M_{AY} = M_{BY} = -F_{CA}\ lp/8$, Therefore: Σ Moments on the structure relative to the axe $Ay = 1/4 * lp * F_{CA}$.

Any calculation done

$$\overline{\overline{I_y^S}} \frac{2}{l_P} \frac{d^2z}{dt^2} = \frac{l_P}{4} F_{CA} = \frac{l_P}{4} S_S \frac{\pi^2 \hbar c}{240} \frac{1}{z^4} \tag{14}$$

with I_{Sy} the inertia of the structure relatively to the axe Ay. See Eq. (14) below.

$$\overline{\overline{I_y^S}} = \rho_P a_{Pb_P l_P} \left(\frac{l_P^2 + a_P^2}{12} + \frac{l_P^2 + a_P^2}{4} \right) + \rho_I a_{ib_i l_i} \left(\frac{l_i^2 + a_i^2}{12} + \frac{(l_P + l_i)^2 + (a_P + a_i)^2}{4} \right)$$

$$+ \rho_S a_{Sb_S l_S} \left(\frac{l_S^2 + a_S^2}{12} + \frac{(l_P + l_i + l_S)^2 + (a_P + a_i + a_S)^2}{4} \right)$$

$$\tag{15}$$

with ρ_P, ρ_I, ρ_S, respectively the densities of the piezoelectric bridge, the intermediate finger and the mobile electrode of the Casimir reflector.

We then obtain the differential equation which makes it possible to calculate the interval between the two electrodes of the Casimir reflector as a function of time during the "descent" phase when the Coulomb forces are not present.

$$\frac{d^2z}{dt^2} = \frac{l_P^2}{8 \; . I_Y^S} \; S_S \; \frac{\pi^2 \hbar c}{240} \frac{1}{z^4} = \frac{B}{z^4} \quad with \; B = \frac{l_P^2}{8 I_Y^S} S_S \frac{\pi^2 \hbar c}{240} \qquad (16)$$

Coulomb forces do not intervene yet because the MOS switches in parallel of circuit 1—before the inductance Lin—are open and the MOS switches in series of circuit 2—after the inductance L_{in}—being closed, the return Coulomb electrode is to earth. The fixed Casimir electrode is always to earth (see **Figures 3** and **5**). Coulomb forces will intervene when the gate voltage $V_G = Q_{mp2\;MOS}/C_{OX}$ on the MOSs of circuit n°1 exceeds the threshold voltage of one of them and when circuit n°2 of the depleted N and P MOSs in series will be open (**Figures 3** and **5**)! Then the switches of the circuit of the parallel MOS transistors will close.

The switches of the series MOS circuit will open and the charge Q_{mn1} initially present exclusively on the electrode of the bridge and of the metallic block will be distributed uniformly over the second part of coulomb electrodes according to:

$$Q_{mn1f} = Q_{mn1} \frac{S_{P1}}{S_{P1} + S_R} \approx \frac{Q_{mn1}}{2}.$$

Because $S_r = S_{p1}$, Just at the moment of closing circuit n°1 and opening circuit n°2 (**Figure 5**) we have $F_{CO} = -p \; F_{CA}$ with p a coefficient of proportionality ≥ 2 defined by the threshold voltages of the MOS interrupters. The total force F_T exerted in the middle of the piezoelectric bridge just at the start of the charge transfer becomes $F_T = F_{CA} - F_{CO} = F_{CA} - p^* \; F_{CA} = F_{CA} \; (1-p)$.

The "descent" time of the free Casimir electrode will therefore stop when $F_{CO} = -p \; F_{CA}$.

However, we know that: $F_{ca} = S\left(\frac{\pi^2 \hbar c}{240 z_S^4}\right)$

1. The Casimir force is variable in time and its equation is Eq. (1):

2. The mobile charge on the Casimir electrodes variable also in time (Eq. (3)) is:

$$Qmn2 \approx \frac{Qmn}{2} = \frac{d_{31} F_{CA} l_P}{2 a_P}$$

3. The Coulomb force (4), variable over time, acting in opposition to the Casimir force (Eq. (4)):

$$F_{CO} = p F_{CA} \Rightarrow \left(S_S \frac{\pi^2 \hbar c}{240} \frac{d_{31} l_P}{2^* a_P} \left(\frac{1}{z_s^4} - \frac{1}{z_0^4} \right) \right)^2 \left(\frac{1}{4\pi\varepsilon_0 \varepsilon_r} \right) \left(\frac{1}{z_r + z_0 - z_S} \right)^2 = p S_S \frac{\pi^2 \hbar c}{240} \frac{1}{z_s^4}$$

The differential Eq. (15) unfortunately does not have a literal solution and we programmed on MATLAB the solution of this differential equation "descent"

and calculated the duration of this "descent" of free Casimir electrode. The duration of the "descent" depending on the desired value of the coefficient of proportionality p, which is regulated by the values of the threshold voltages of the MOS transistors and defined during the manufacture of the device. The "descent" of the free Casimir electrode stops when the inter electrode interface z_s is such that:

$$z_s^4\left(\left(\frac{1}{z_r+z_0-z_S}\right)^2\left(\frac{1}{z_S^4}-\frac{1}{z_0^4}\right)\right)=p\frac{3840\pi\varepsilon_0\varepsilon_r}{\pi^2\hbar cS_S}\left(\frac{a_P}{d_{31}l_P}\right)^2 \qquad (17)$$

This programmable equation gives the time t_d of the "descent" of the structure submitted to the Casimir force and:

a. depend on the coefficient of proportionality p,

$$F_T=(1-p)F_{CA}\Rightarrow(1-p)S_S\frac{\pi^2\hbar c}{240}\frac{1}{z_{sm}^4}<0\quad if\,p>1$$

b. is calculable and will stop when the inter-electrode interface z_s has a value z_{sm} satisfying Eq. (16). At the instant of the appearance of the Coulomb force, with z_{sm} the value solving 16, the total force is therefore:

1. The total force, variable over time and exerted at the center of the piezoelectric bridge, becomes (Eq. (17)):

$$F_T=F_{CA}-F_{CO}$$
$$=S_S\left(\frac{\pi^2\hbar\ c}{240}\right)\left(\frac{1}{z_s^4}-S_S\frac{\pi^2\ \hbar\ c}{240}\left(\frac{d_{3\ 1}\ l_P}{a_P}\right)^2\right)\left(\frac{1}{16\ \pi\ \varepsilon_0\ \varepsilon_r}\right)\left(\frac{1}{z_s^4}-\frac{1}{z_s^4}\right)^2\left(\frac{1}{(z_r+z_0-z_S)^2}\right)$$
$$(18)$$

The piezoelectric bridge subjected to this force then rises towards its neutral position. The Casimir inter electrode interval increases causing the Casimir force to decrease! As the deformations of the piezoelectric bridge decrease, the electric charge present on the piezoelectric face's decreases, which consequently leads to a drop in the Coulomb Force. The F_T force therefore rapidly approaches the starting F_{CA} force, during the "ascent" of the Casimir electrodes.

Let us calculate the duration of this "rise" of the mobile electrode of the Casimir reflector triggered when $F_{CO}=p^*\,F_{CA}$.

To know the time taken by the structure to "go back" to its neutral position, we must solve the following differential equation (Eq. (18)):

$$\frac{d^2z}{dt^2}=\frac{l_P^2}{8.I_Y^S}(F_{CA}-F_{CO})$$
$$=\frac{l_P^2}{8.I_Y^S}\left(lsb_S\frac{\pi^2\hbar c}{240}\frac{1}{z_s^4}-lsb_S\frac{\pi^2\hbar c}{240}\frac{d_{31}l_P}{2^*a_P}\frac{1}{4\pi\varepsilon_0\varepsilon_r}\left(\frac{1}{z_s^4}-\frac{1}{z_0^4}\right)^2\left(\frac{1}{z_r+z_0-z_S}\right)^2\right)$$

By posing $A1=lsb_S\left(\frac{\pi^2\hbar c}{240}\right)$ the differential Eq. (17) concerning the "ascent" of the bridge is written:

$$\frac{d^2z}{dt^2} = \frac{l_P^2}{8.\ I_Y^S}(F_{CA} - F_{CO})$$

$$= \frac{l_P^2}{8.\ I_Y^S} A1 \left(\frac{1}{z_s^4} - A1\left(\frac{d_{3\ 1}l_P}{a_P}\right)^2\right)\left(\frac{1}{16\ \pi\ \varepsilon_0\ \varepsilon_r}\right)\left(\frac{1}{z_s^4} - \frac{1}{z_0^4}\right)^2\left(\frac{1}{(z_r + z_0 - z_S)^2}\right)$$

$$(19)$$

This differential Eq. (18) has no analytical solution and can only be solved numerically. We programmed it on MATLAB with the inter-electrode distance z_s belonging to the interval $[z_{sm}, z_0]$. The properties and dimensions of the different materials used in this simulation are as follows (**Table 1**).

The metal used for the Casimir reflector block is Aluminum with a density of $2.7\ \mathrm{g\ cm^{-3}}$.

In these MATLAB calculations we considered that the metal of the electrodes and metal block was oxidized over a thickness allowing to have an interface between Casimir electrodes of 200 A° (see Chapter 5) which modifies the mass and the inertia of the vibrating structure. It turns out that the choice of aluminum as the metal deposited on these electrodes is preferable given:

1. The ratios between the thickness of the metal oxide obtained and that of the metal attacked by the growth of this oxide during its thermal oxidation (see Chapter V).

	PZT	AlN	LiNbO3	PMN-PT: (1-x) Pb(Mg1/3−Nb1/3)O3-xPbTiO3
Young Modulus $(\mathbf{kg^*\,m^*\,s^{-2}})/\mathbf{m^2}$	Ep = 8.9*10^{10}	Ep = 32*10^{10}	Ep = 2.45*10^9	Ep = 150*10^9
Volumic mass $(\mathbf{kg\ m^{-3}})$	dp = 7600	dp = 3255	dp = 4700	dp = 7920
Piezoelectric coefficient d31 of the beam $(\mathbf{C/(kg^*\ m^*\ s^{-2})})$	d31 = 200*10^{-12}	d31 = 2.400*10^{-12}	d31 = 6*10^{-12}	d31 = 1450*10^{-12}
Length piezoelectric beam lp (m)	50 10^{-6}	50 10^{-6}	50 10^{-6}	50 10^{-6}
Width piezoelectric beam bp (m)	150 10^{-6}	150 10^{-6}	150 10^{-6}	150 10^{-6}
Thickness piezoelectric ap (m)	10 10^{-6}	10 10^{-6}	10 10^{-6}	10 10^{-6}
Connecting finger length li (m)	10 10^{-6}	10 10^{-6}	10 10^{-6}	10 10^{-6}
Width finger connection bi (m)	150 10^{-6}	150 10^{-6}	150 10^{-6}	150 10^{-6}
Thickness finger connection ai (m)	10 10^{-6}	10 10^{-6}	10 10^{-6}	10 10^{-6}
Mobile Casimir electrode block length ls (m)	500 10^{-6}	500 10^{-6}	500 10^{-6}	500 10^{-6}
Mobile Casimir electrode block width bs (m)	150 10^{-6}	150 10^{-6}	150 10^{-6}	150 10^{-6}
Casimir mobile electrode block thickness as (m)	10 10^{-6}	10 10^{-6}	10 10^{-6}	10 10^{-6}

Table 1.
Table of characteristics used for MATLAB and ANSYS simulations.
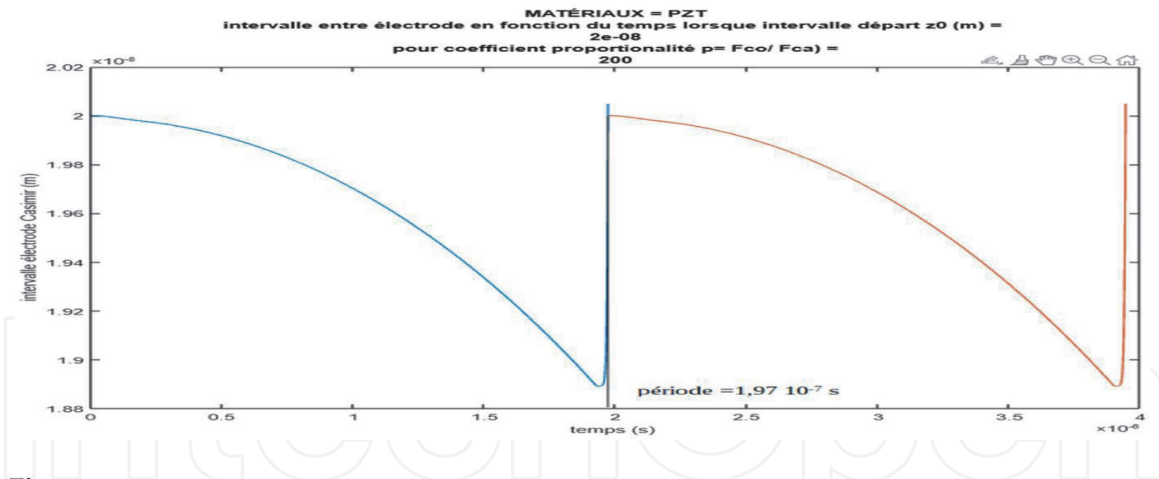
Figure 12.
Vibrations of the structure for a coefficient of proportionality p = FCO / FCA = 200: PZT.

2. As its density is weak, we chose aluminum for the purpose to increasing and optimizing the vibration frequency of the structure by minimizing the inertia of the Casimir's reflector and parallelepiped block transferring the Casimir force to the piezoelectric bridge. The mass M of the vibrating structure is then:

$$M = d_{pm} * (a_s * b_s * l_s + a_i * b_i * l_i) + d_{om} * 2 * z_{of} * (a_{so} * b_{so} + b_{so} * l_{so} + a_{so} * l_{so)} + d_p * (a_p * b_p * l_p);$$

With d_{pm} the density of the metal, a_s, b_s, l_s the geometries of the final metal part of the Casimir electrode sole, d_{om} the density of the metal oxide, a_{so}, b_{so}, l_{so} the geometries of the oxidized parts around the 6 faces of the metal block, dp the density of the piezoelectric parallelepiped (see **Figure 12**):

3.2 Calculation of the current peak

Let us estimate the duration of the current peak linked to the circulation and homogenization on the return electrodes of the mobile charges. Let R_m be the ohmic resistance of the metals used for the surface electrodes S_{p1} + the L_{IN} solenoid + the S_r electrode (see **Figure 3**) and Cs the capacitance formed by the gap between the return electrodes Sp2 and S_r. Then the current peak circulating during the transition of the mobile loads between Sp1 to S_R via circuit n°1 and the L_{IN} solenoid is, as we have seen:

$$I_{IN} = \frac{Q_{mn2}}{R_m C_S} Exp \left(-\frac{t}{R_m C_S} \right)$$

The time t being counted from the closing of the MOSNE switch. The duration of this current peak is estimated at $t_e = R_m.C_s$. Log (2), when the charges on each electrode will be $Q_{mn2}/2$. This current peak is present even if the switch transistors may close some time after, because the mobile charges have already propagated.

- $R_m \cong r_m * l_m/S_m$, with ρ_m the resistivity of the metallic conductor in the circuit between electrodes (the solenoid + the electrodes themselves), l_m its total length of this conductor, S_m its section

- $Cs = \varepsilon_0.\varepsilon_{om}.l_p.b_p/z_r$, the inter-electrode return capacitance, with ε_0 the permittivity of vacuum, v the relative permittivity of the metal oxide, l_p and b_p the geometries of the return electrode. A calculation of the duration of the homogenization of the electric charges and therefore of the duration of the

current peak (based on an estimate to propagate in a L_{IN} coil of about 10^{-5} Henri) gives $t_e \cong 10^{-9}$s. This current peak, passing through a L_{IN} solenoid develops a voltage peak $U_{IN} = L_{IN} I_{INP}/t_e = L_{IN} * Q_{mn2}/(2.te * R_m.C_s)$ which will be exploited by integrated electronics without any power supply described in Chapter IV.

We present below the results of the MATLAB simulations carried out by numerically calculating the differential Eqs. (15) and (18). These numerical calculations give the vibration frequency of the structure which, as we will see, vibrates at a frequency lower than its first resonant frequency (IV).

This vibration frequency depends on the characteristics of the structure (Nature of the piezoelectric material, nature of the metallic conductors, initial interface z_0 and z_r between Casimir electrodes and return electrodes, geometric dimensions of the Casimir reflectors, coefficient of proportionality $p = F_{CO}/F_{CA}$ ...)) (See IV and Annex).

4. Simulation of devices with different piezoelectric bridge

We will see that this device vibrates at a frequency lower than its first resonant frequency and that its vibration frequency depends on the characteristics of the structure (Nature of the piezoelectric material, nature of the metallic conductors, starting interface z_0 and z_r between Casimir electrodes and return Coulomb electrodes, dimensions of the Casimir reflectors, coefficient of proportionality $p = F_{CO}/F_{CA}$ ...). Except precision the interface z_r between the Coulomb's electrode is chosen the same that those of Casimir reflector z_0

4.1 Piezoelectric materials = PZT (lead zirconia titanium)

4.1.1 Interface between Casimir electrodes as a function of time for different trigger values of MOS transistors

For a starting interface between Casimir electrode of $z_0 = 200 * 10^{-10}$ (m) and a coefficient of proportionality $p = F_{CO}/F_{CA} = 2$, we obtain the following evolution in time of the Casimir interface:

We notice a phase of rise of the Casimir electrode faster than that of descent. The period of vibrations is $6.18 \ 10^{-7}$ s therefore with a vibration frequency of $1.613 \ 10^6$ Hertz, while the first resonant frequency of the same structure is $6.54 \ 10^6$ hertz.

The moving electrode drops to $z_s = 198.8$ Angstroms from the fixed electrode S_{S3}. The current peak for this coefficient of proportionality $p = 2$ is $2.58 \ 10^{-8}$ A. This current is obtained by adjusting the threshold voltage of the enriched and depleted MOS transistors to a value Vt = 0.6553 V for a length L = width = W = 4 10^{-6} m and with a grid oxide thickness SiO2 = tox of $250 \ 10^{-10}$ m (see **Figure 13**)! Let us simply change the coefficient $p = F_{CO}/F_{CA}$ of proportionality to p = 200, then we get (see **Figure 14**):

We notice for the ratio $p = F_{CA}/F_{CO} = 200$ (**Figure 14**), a phase of "rise" of the Casimir electrode also much faster than that of "descent" but also more dynamic than for the ratio of previous p = 2 The vibration frequency of the device of $5.07 \ 10^5$ hertz, while the first resonant frequency of the structure is still $6.54 \ 10^6$ hertz!

The moving electrode is now approaching to $z_s = 188.9 A°$ of the fixed electrode S_{S3}, so the vibration amplitude of the structure is 200–188.9 = 11.1 Angstroms!

This current is obtained by adjusting the threshold voltage of the enriched and depleted MOS transistors to a value Vt = 6.89 V for the same geometries as above
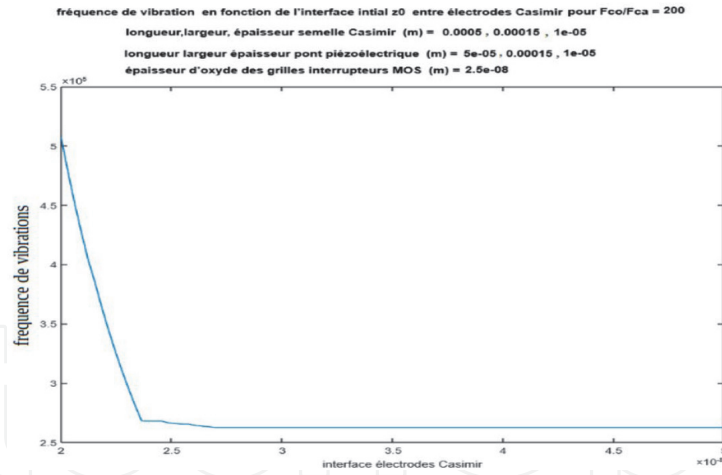
Figure 13.
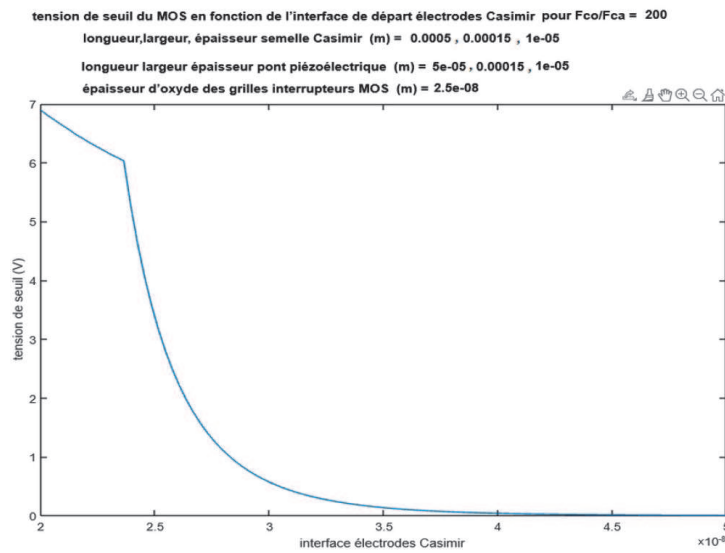*Structure vibration frequency = f (starting interface z0): F_{CO} / F_{CA} chosen = 200: PZT.*

Figure 14.
MOS threshold voltage = f (starting interface z0): F_{CO} / F_{CA} chosen = 200: PZT.
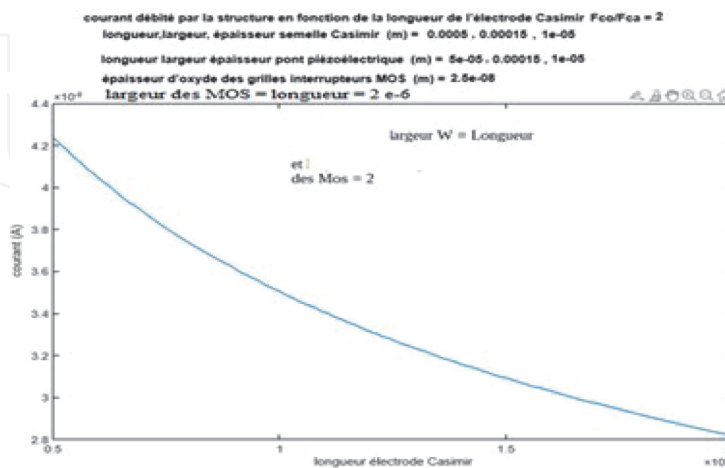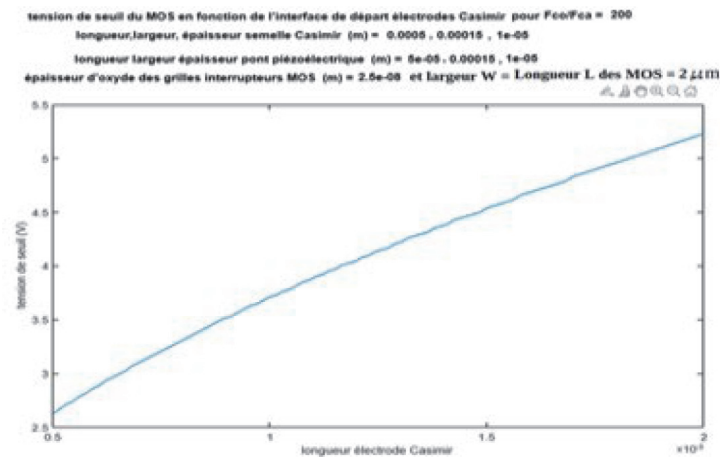

Figure 15.
Maximum current = f (length of the Casimir electrode ls), starting interface = 200 A °, selected coefficient of proportionality p = F_{CO} / F_{CA} = 2.
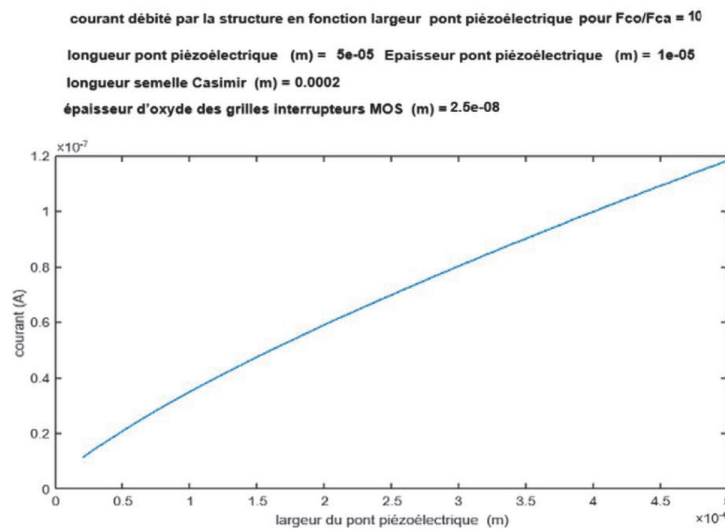
(see **Figure 15**). We must therefore adjust the threshold voltages to precisely adjust the ratio p = F_{CO}/F_{CA} for which the Coulomb force is triggered. This is a point that can be easily obtained technologically (see the technological part of this report)! In

conclusion, as the vibration frequency of the structure depends, among other things, on the coefficient of proportionality p and therefore on the current that one wishes to obtain, *the structure does not vibrate at its first resonant frequency*.

4.1.2 Variation of the starting interface z_0 between Casimir electrodes: PZT

We notice (**Figure 16**) that the vibration frequency of the structure drops as the initial space between the Casimir electrodes increases, which is related to a decrease in the Casimir Force and therefore makes sense. The vibration frequency depends on the chosen F_{CO}/F_{CA} ratio. This frequency drops and stabilizes around 2.6 MHz as the electrode interface increases by a ratio of 200. It is much lower than the first resonant frequency of the structure which is 6.85 Megahertz (for this structure). The vibration frequency approaches that of first resonance if the starting z_0 interface is less than 200 Angstroms.

We chose an initial interface of 200 A° for reasons of technological feasibility (see VI)!

We also notice (**Figure 17**) that the threshold voltage of the Enriched and Depleted MOS transistors increases with a decrease in the starting interface

Figure 16.
Threshold Voltage = f (length of the casimir electrode ls), starting interface = 200 A °, selected coefficient of proportionality p = F_{CO} / F_{CA} = 2.
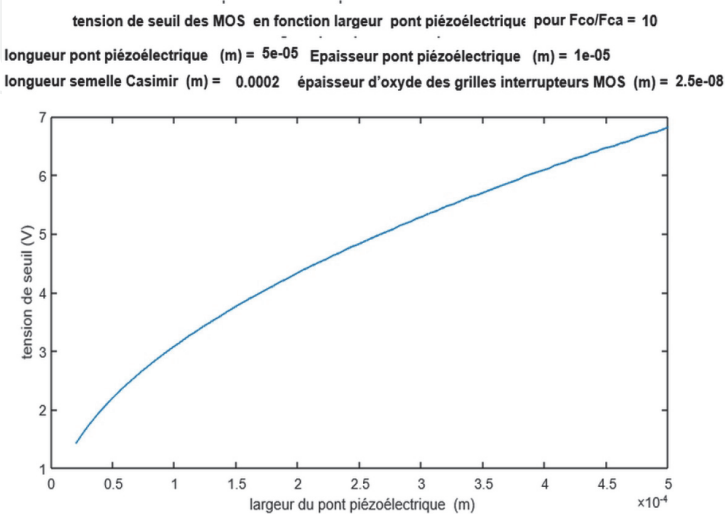
Figure 17.
Threshold voltage of the MOS = f (width of the casimir electrode bp), starting interface = 200 A °, selected coefficient of proportionality = p = F_{CO} / F_{CA} = 10.
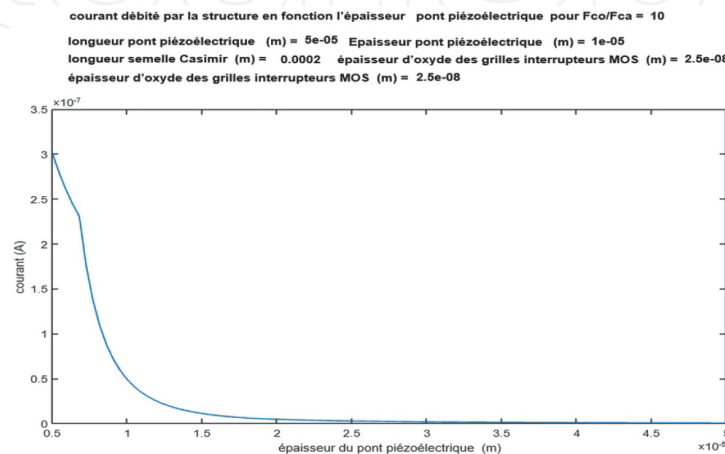
between Casimir electrodes. This seems logical, since the Casimir force increasing, the deflection of the bridge and therefore the charges generated on its faces do the same. It is therefore necessary that the threshold voltage of the MOS transistors be greater so that the voltage V_G on the gates of the MOS does not trigger them!!

4.1.3 Current and threshold voltage function of the length ls of the Casimir electrode: PZT

We obtain (**Figure 18**) a small decrease in current with the increase in the length of this electrode. However, a significant increase in the threshold voltage (**Figure 19**), which is understandable since the inertia of the structure increases.
We obtain (**Figure 18**) a small decrease in current with the increase in the length of this electrode and a significant increase in the threshold voltage (**Figure 19**), which is understandable since the inertia of the structure increases.

4.1.4 Variation of the width bp of the piezoelectric bridge: PZT

We now vary the width b_p of the piezoelectric bridge. We obtain an increase in the threshold voltage of the MOS by increasing the width b_p of the piezoelectric

courant débité par la structure en fonction largeur pont piézoélectrique pour Fco/Fca = 10

longueur pont piézoélectrique (m) = 5e-05 Epaisseur pont piézoélectrique (m) = 1e-05

longueur semelle Casimir (m) = 0.0002

épaisseur d'oxyde des grilles interrupteurs MOS (m) = 2.5e-08

Figure 18.
Maximum current = f (width of the casimir electrode bp), starting interface = 200 A °, selected coefficient of proportionality = p = F_{CO} / F_{CA} = 10.

courant débité par la structure en fonction l'épaisseur pont piézoélectrique pour Fco/Fca = 10

longueur pont piézoélectrique (m) = 5e-05 Epaisseur pont piézoélectrique (m) = 1e-05

longueur semelle Casimir (m) = 0.0002 épaisseur d'oxyde des grilles interrupteurs MOS (m) = 2.5e-08

épaisseur d'oxyde des grilles interrupteurs MOS (m) = 2.5e-08

Figure 19.
Current of the MOS = f (Thickness of piezoelectric film ap), start Interface = 200 A ° with a choice F_{CO} / F_{CA} =10.
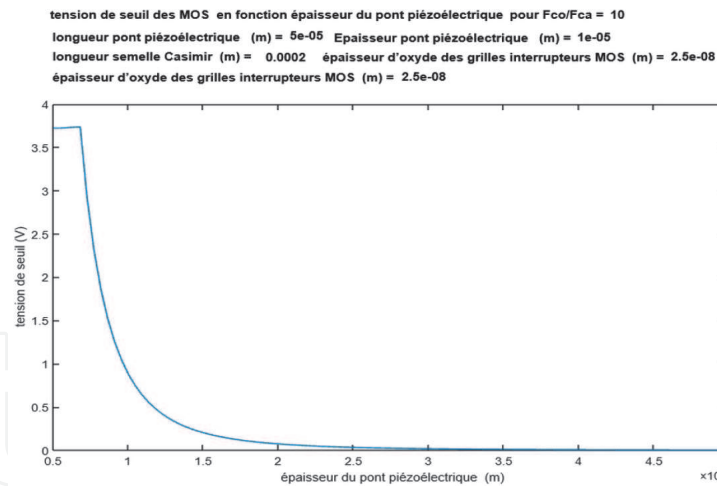
Figure 20.
Threshold of the MOS = f (Thickness of piezoelectric film ap), start Interface = 200 A ° with a choice F_{CO} / F_{CA} =10.
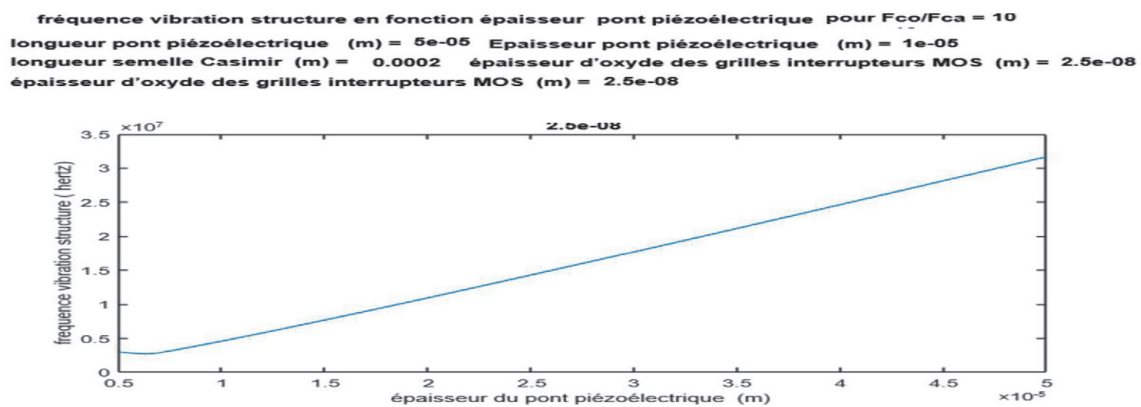
Figure 21.
Structure vibration frequency as a function of the thickness ap of the piezoelectric bridge, starting interface z0 to 200 A °, Ratio p = F_{CO} / F_{CA} = 10.

bridge. However, the current delivered by the structure varies little with the width of the piezoelectric bridge (**Figures 20** and **21**). These considerations give that:

For reasons of technological convenience, it will be preferable to choose a thickness of around 20 μm!

4.1.5 Variation of the thickness ap of the piezoelectric bridge: PZT

If we increase the thickness a_p of the piezoelectric bridge, we obtain a decrease in the current (**Figure 22**) and of the threshold voltage of the MOS (**Figure 23**), but an increase in the vibration frequency (**Figure 24**).

The vibration frequency increases linearly with the thickness of the piezoelectric bridge (**Figure 25**).

4.1.6 Variation of the proportionality ratio $\mathbf{p} = \mathbf{F_{CO}}/\mathbf{F_{CA}}$: PZT

In a non-intuitive way, the current simply increases linearly by a factor of 40 (**Figure 26**) if we increase the proportionality ratio p = F_{CO}/F_{CA} by a factor of 500. On the other hand, the threshold voltage of the MOS switches increases by a factor 8 for the same variation of the interface (**Figure 27**).
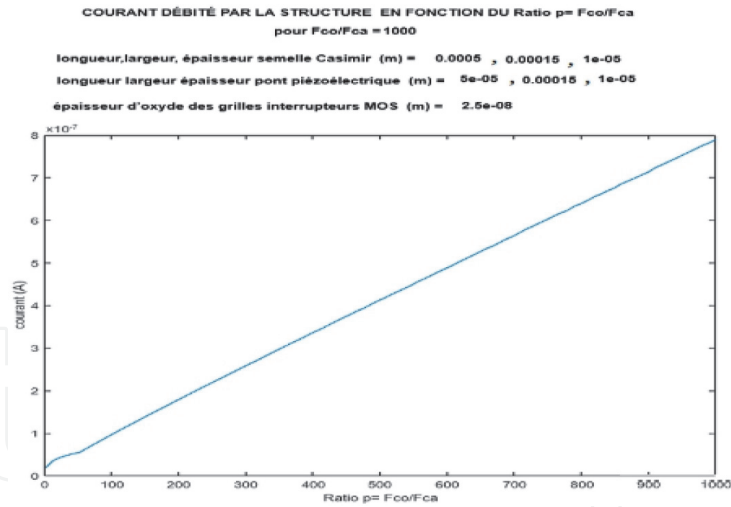
Figure 22.
Current of the MOS = f (ratio = F_{CO} / F_{CA}), start Interface = 200 A ° piezoelectric material = PZT.
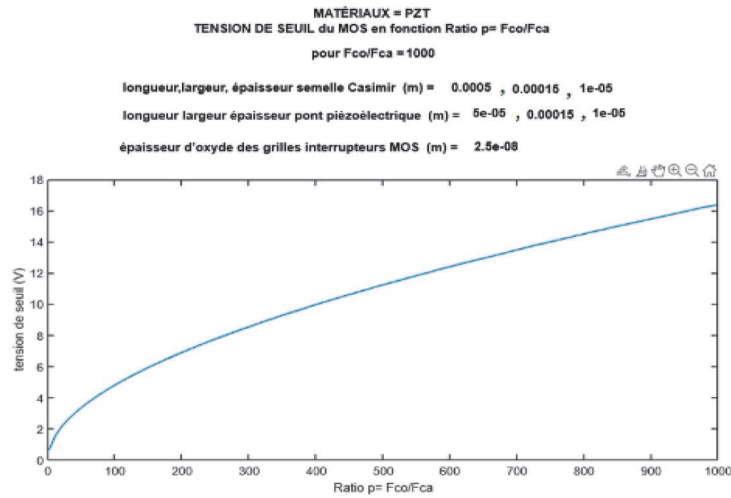
Figure 23.
Threshold voltage of the MOS = f (ratio = F_{CO} / F_{CA}), start Interface = 200 A ° piezoelectric material = PZT.
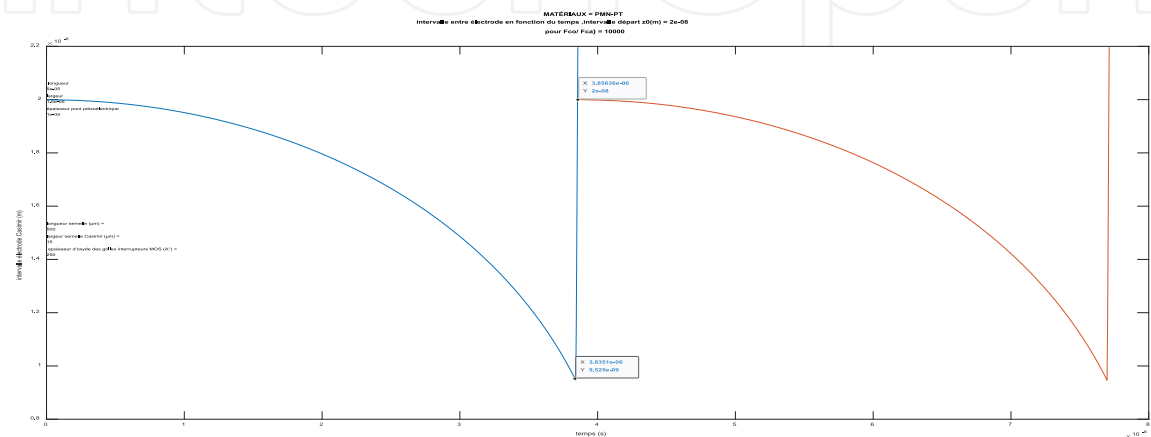
Figure 24.
Plot of the evolution of the Casimir inter-electrode interval as a function of time over two periods and an F_{CO} / F_{CA} ratio = 1000: Casimir inter-electrode interface = 200 A°.
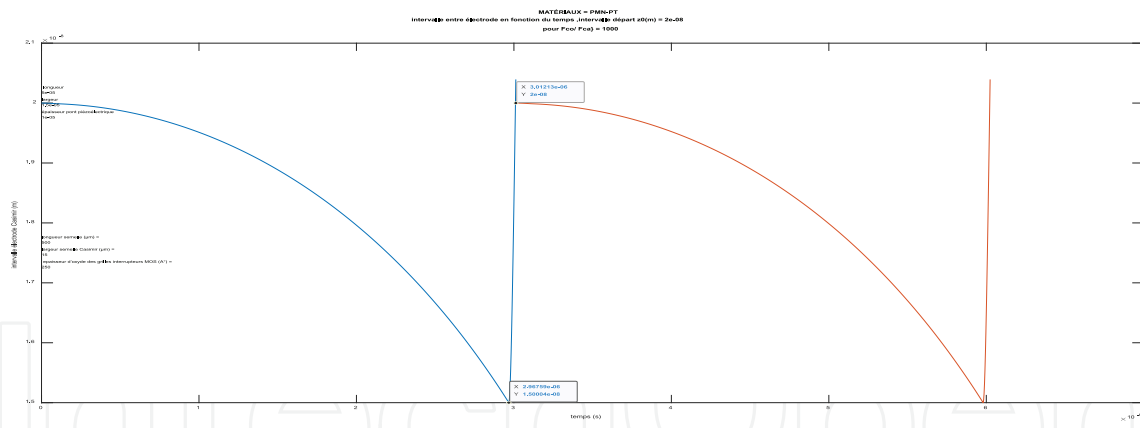
Figure 25.
Plot of the evolution of the Casimir inter-electrode interval as a function of time over two periods and an F_{CO} / F_{CA} Ratio = 1000: Casimir inter-electrode interface = 200 A °.
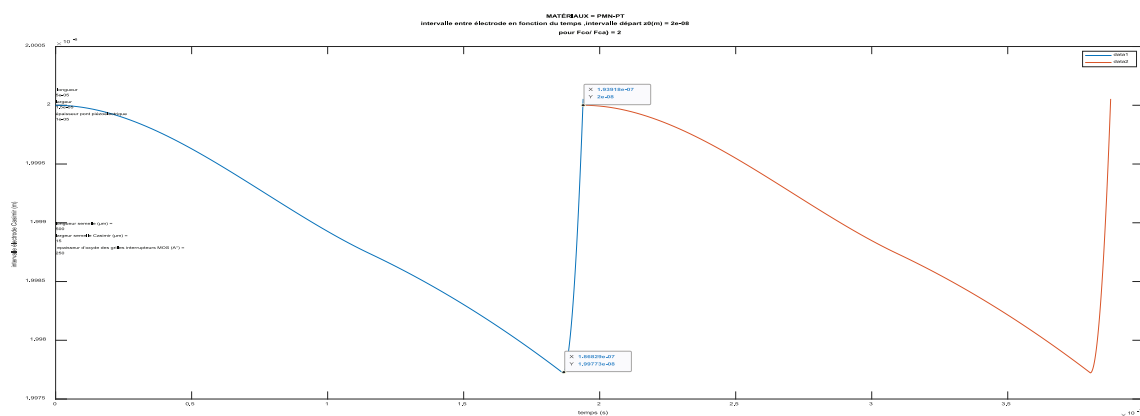
Figure 26.
Plot of the evolution of the Casimir inter-electrode interval as a function of time over two periods and a ratio F_{CO} / F_{CA} = 2. Casimir inter-electrode interface = 200 A °.
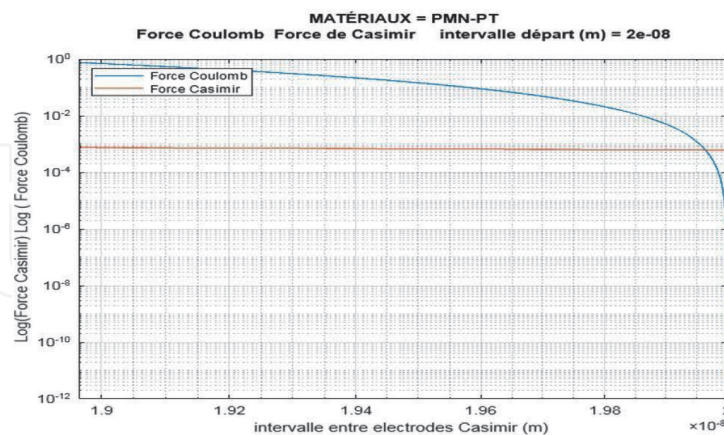
Figure 27.
Materials = PMN-PT: Coulomb and Casimir force as a function of the inter-electrode interface. Start interface = 200 A °.

The MOS N or P switch transistors enriched in parallel have the following geometries: Width W = 4 mm and length L = 4 mm

4.2 Use of other piezoelectric materials

In the presentation above we used PZT but, in order to increase the density of electric charges at the terminals of the piezoelectric bridge, piezoelectric material
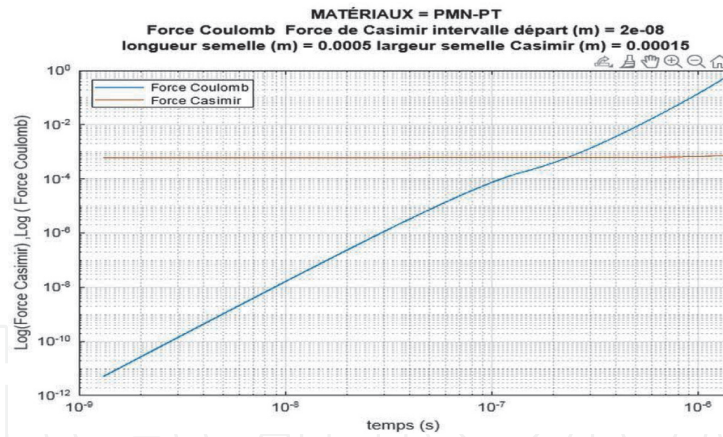
Figure 28.
Materials = PMN-PT: Coulomb and Casimir force as a function of time. Start interface = 200 A °.

PMN-PT can be used which can be deposited by RF-magnetron sputtering and of composition, for example: PMN-PT = (1-x) Pb (Mg1/3 − Nb1/3) O3-xPbTiO3; $d_{31} = 1450^* 10^{-12} C/(kg^* m^* s^{-2})$ and a Young's modulus of $Ep = 150^* 10^9$ (**Figure 28**). We will also simulate the results obtained with AlN (aluminum nitride) $(d_{31} = 2.4^* 10^{-12} et\ Ep = Ep = 32^* 10^{10})$, another piezoelectric material or AlN widely used in microelectronics because it is easily removable and lead-free!

4.2.1 Piezoelectric material = PMN-PT

With the MATLAB simulation of a structure using PMN-Pt we obtain the evolution over time of the Casimir and Coulomb forces as well as the F_{CO}/F_{CA} ratio of **Figures 7, 11, 13, 24, 29–39** below. For a ratio of 1000, the maximum current delivered by the vibrating structure, the threshold voltage of the MOSE and MOSD and the vibration frequency of the structure are respectively: $1.2\ 10^{-4} A$, Vt = 3.2 V and 957,000 Hertz

4.2.1.1 Evolution of the Casimir interface as a function of time during two periods: PMN-PT

The F_{CO}/F_{CA} ratio = 10,000 induces a period of $3.85\ 10^{-6}$ s and a rise time of $21.3\ 10^{-9}$ s with a deflection of the bridge of 105 A°. The structure vibrates at
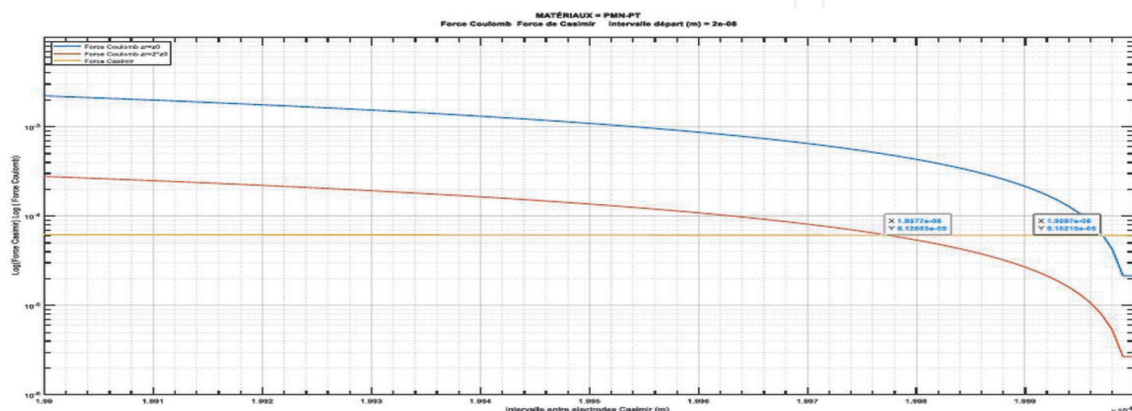
Figure 29.
Materials = PMN-PT: Coulomb force for zr = 200 A ° (Blue)and zr = 400 A ° (Red) and Casimir force (Yellow , z0 =200 A °) as a function of the inter-electrode interface Starting interface = 200 A °.
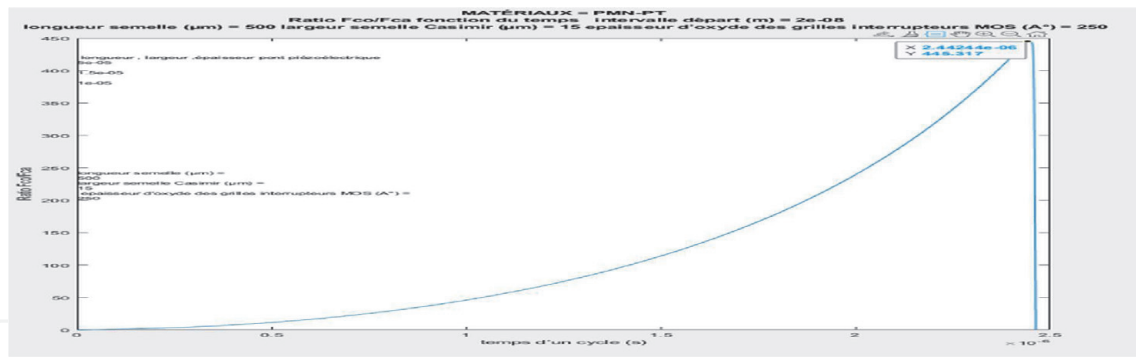
Figure 30.
Materials = PMN-PT: Ratio p = F_{CO} / F_{CA} as a function of time. During a period of vibration. Start interface = 200 A °, Maximum ratio chosen = 450 A °.

259.7 kHz. At the rise sequence, the structure exceeds the initial 200 A° by 20 A° due to inertia (**Figure 29**).

The ratio F_{CO}/F_{CA} = 1000 induces a period of $2.96 \ 10^{-6}$ s and a rise time of $44.5 \ 10^{-9}$ s with a deflection of the bridge of 50 A° The structure vibrates at 337.8 kHz.

For p = 1000 (**Figure 24**), we notice a vibration amplitude of 50 A° with a period of $2.96 \ 10^{-6}$ s, with faster rise of the mobile electrode producing a slight rebound of 5A, because of the inertia of the structure.

For the ratio $F_{CO}/F_{CA} = 2$ (**Figure 30**) a vibration amplitude of just 0.27 A° and a period of $1.86 10^{-7}$ s is obtained This low deformation of the PMN-PT piezoelectric bridge is mainly due to the extremely high piezoelectric coefficient d_{31} of 1450 (pC/N) of PMN-PT compared to 120 (pC/N) for PZT (**Figure 28**). It is also observed that weak overshoot of the initial interface (200 A°) for the mobile electrode increases with the ratio (F_{CO}/F_{CA}).

4.2.1.2 Evolution of the forces of Casimir and Coulomb: PMN-PT

We obtain the evolution of the Casimir and Coulomb forces as a function of the inter-electrode interface (**Figure 13**) and over time (**Figure 31**) as well as the
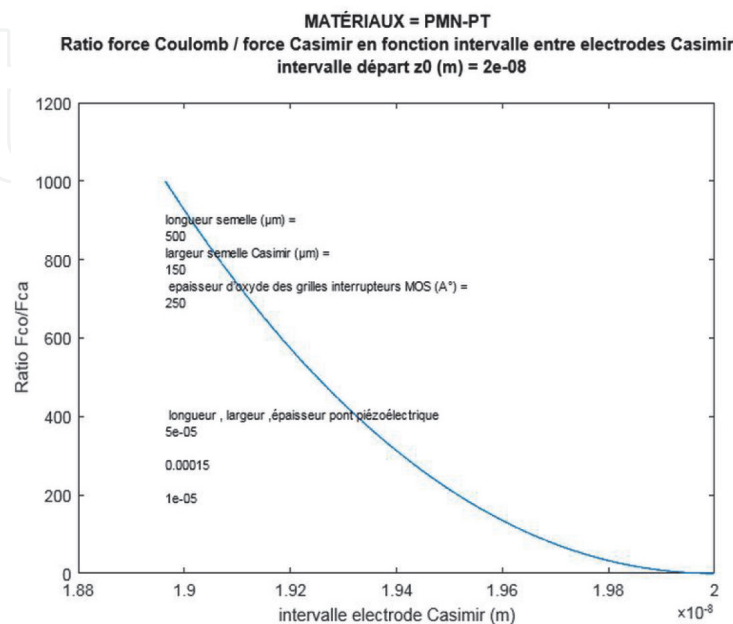
Figure 31.
Materials = PMN-PT: Coulomb Force / Casimir Force ratio as a function of the Casimir inter-electrode interface. Start interface = 200 A °.
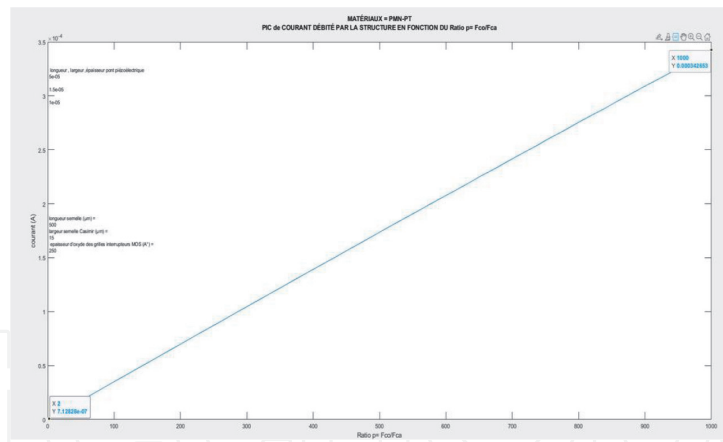
Figure 32.
Materials = PMN-PT: peak current delivered by the structure as a function of the F_{CO} / F_{CA} ratio. Start interface = 200 A °.

F_{CO}/F_{CA} ratio as a function of time for an entire period (**Figure 7**). For an interval between Casimir electrode z_0 = 200 Angstroms, we observe (**Figure 7**) that the Coulomb return force becomes more important than the Casimir force, if we induce a deflection of the piezoelectric bridge of 20 A° more for an interval z_r = 400 Angstroms between return electrodes than for z_r = 200 that.

The attraction of the electrodes by the Casimir force induces a deformation of the piezoelectric bridge, therefore electric charges, which can be used in the Coulomb force. The break circuits triggered at time t = 2.44 10^{-6} s suddenly induce a rise of the mobile electrode, therefore a sudden decrease in electric charges. We observe the gradual evolution towards the chosen ratio of 450 and then the sudden drop in this ratio as the electrodes regain their initial position (**Figure 32**).

4.2.1.3 Ratio as a function of Casimir interval and current peak as a function of the ratio: PMN-PT

We observe (**Figure 33**) that for PMN-PT a deflection of 10 A° and a length of the piezoelectric bridge of 150 μm of the mobile Casimir electrode is sufficient to have an Fco/Fca ratio = 1000. A Ratio of 2 gives a peak current of 7 10^{-7} A, while a ratio of 1000 produces a peak current of about 3.5 10^{-4} A (**Figure 34**) for the same period of homogenization of the charges of about 10^{-9} s!
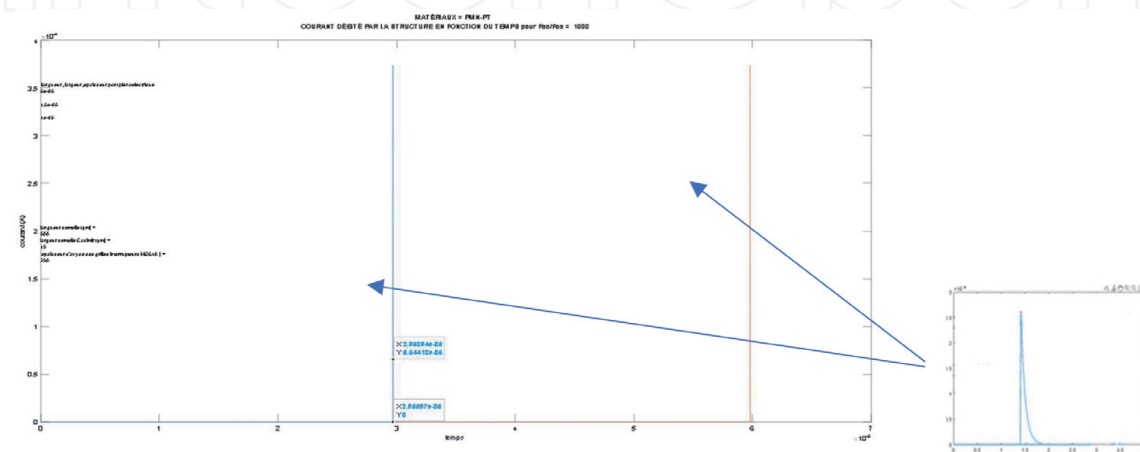
Figure 33.
Materials = PMN-PT: current peak as a function of time obtained over 2 cycles. Starting interface = 200 A °. Ratio p = F_{CO} / F_{CA} = 1000.
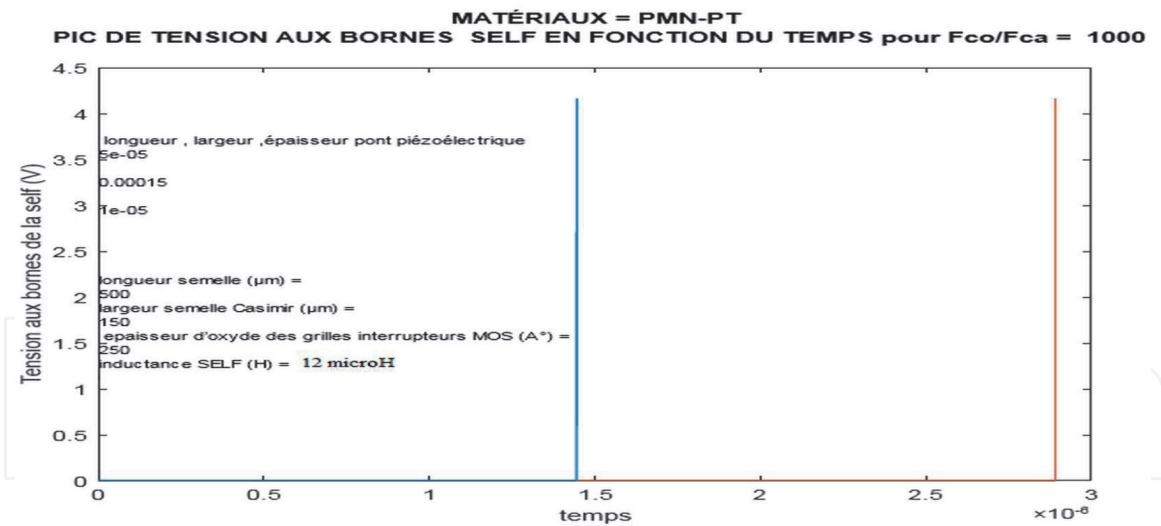
Figure 34.
Materials = PMN-PT: Voltage peak across the $4 * 10^{-5}$ H solenoid as a function of the time obtained over 2 cycles. Starting interface = 200 A °, Ratio p = F_{CO} / F_{CA} = 1000.

4.2.1.4 Peak current as a function of time and peak voltage across the inductance for 2 periods: PMN-PT

The following figures illustrate the peak current generated by the automatic vibrating structure with an inserted magnification showing the shape of this peak as a function of time (**Figure 11**) and its exponentially decrease during about 10–9 s. This current of about 3.5 10–4 A flowing through an inductor L_{IN} of 4 10^{-5} Henri naturally generates a voltage of 4 Volts (**Figure 35**).

Note in **Figure 11** the exponential form of the current peak of a duration appearing in each period. It is the same for the voltage peaks at the terminals of the inductance (**Figure 35**).

As this current peak cross an inductor, it induces by itself a voltage peak.

The current peak that appears with each cycle of vibration is uniquely due to the homogenization of the electrical charges on the two parts of the return electrode. This current peak follows the equation.
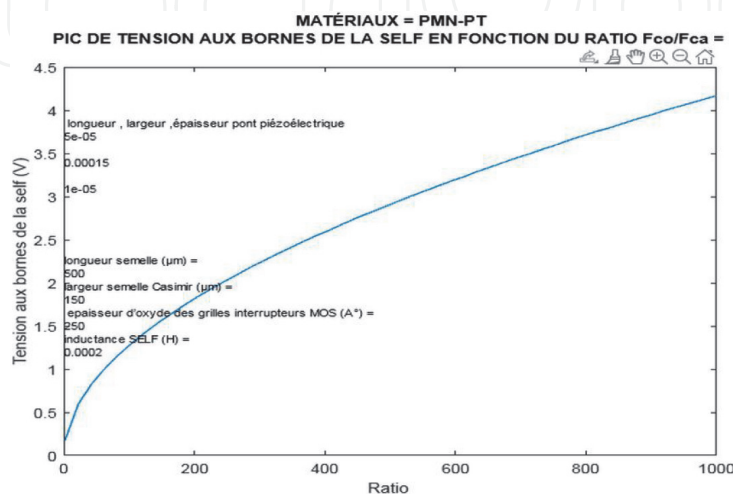
Figure 35.
Materials = PMN-PT: Voltage peak across the $4 * 10^{-5}$ H solenoid as a function of the F_{CO} / F_{CA} Ratio. Start interface = 200 A °.

$$I_{IN} = -\frac{Q_{mn2}}{R_m C_s} \left(Exp\left(-\frac{t}{R_m C_s}\right)\right) \text{ with } Q_{mn2} = d_{31}lp \ F_{CA}{}^* \ a_p/2.$$

This charge transferred from the electrode on the face 1 of the piezoelectric bridge to the return electrode, which is initially grounded, does not depend on the common width bp = bs = bi of the structures. This point is important and facilitates the technological realization of these structures since it limits the difficulties of a deep and straight engraving of the different structures. On the other hand, the intensity of this peak current depends linearly on the lengths lp and ls of the structures (**Figure 22**).

However, the duration of the exponential peak $t_e = R_m C_S \ \ln(2)$ is independent of the geometries of the structure. These only intervening in the frequency of vibration of the structure and in the intensity of the peak.

4.2.1.5 Peak voltage across the inductance and threshold voltage according to the desired FCO/FCA ratio: PMN-PT

We observe (**Figure 36**) that the automatically peak voltage obtained without any energy expenditure increases by a factor of 16 and goes from 0.25 V to 4 V when the ratio $p = F_{CA}/F_{CO}$ increases from 2 to 1000. Likewise, the threshold voltage MOSE and MOSD authorizing these ratios increases from 0.2 V to 3.2 V (**Figure 37**).

4.2.1.6 Vibration frequency as a function of the F_{CO}/F_{CA} ratio and peak current as a function of the initial Casimir interval chosen: PMN-PT

Note (**Figure 38**), that for an initial interface $z_0 = 200$ A°, the maximum vibration frequency of the structure is 3.50 MHz for a ratio Fco/Fca = 2. It falls to 750 kHz for a ratio of 1000. These frequencies remain lower than that of the first resonance of the structure which is the order of 7.94 Megahertz! For an $p = F_{co}/F_{ca}$ ratio = 500, the maximum current delivered by the structure drops as a function of the initial Casimir interval (**Figure 39**).
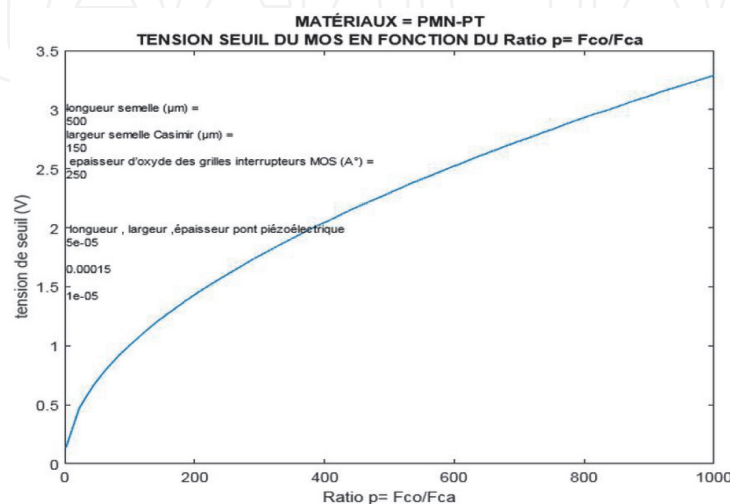

Figure 36.
Materials = PMN-PT: Threshold voltage of the Enriched or Depleted MOTS according to the F_{CO}/F_{CA} ratio. Start interface = 200 A °.
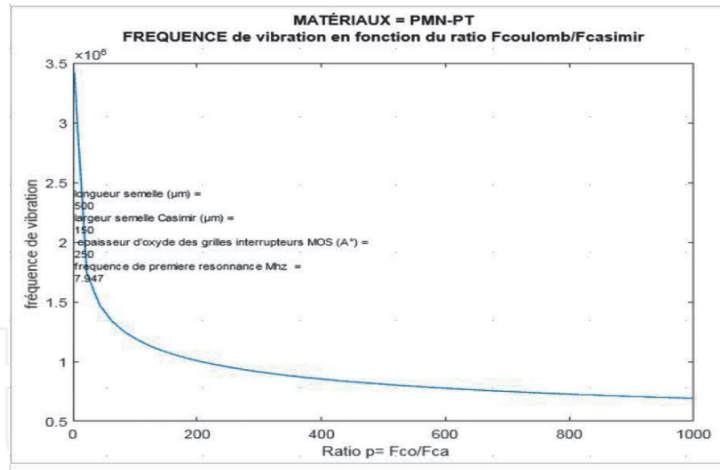
Figure 37.
Materials = PMN-PT: vibration frequency as a function of the F_{CO} / F_{CA} ratio. Start interface = 200 A °. Start interface = 200 A °.
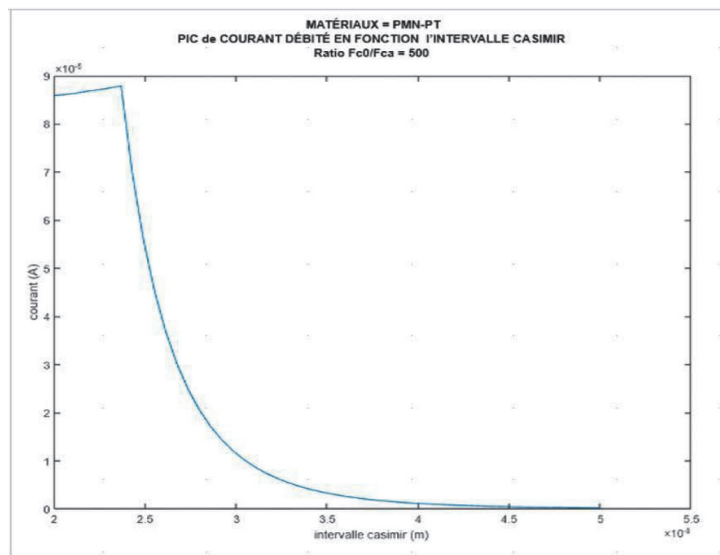

Figure 38.
*Materials = PMN-PT: Current peak across the 2 * 10-4 H inductance as a function of the starting interval between Casimir electrodes. Start interface = 200 A °.*

Figure 39.
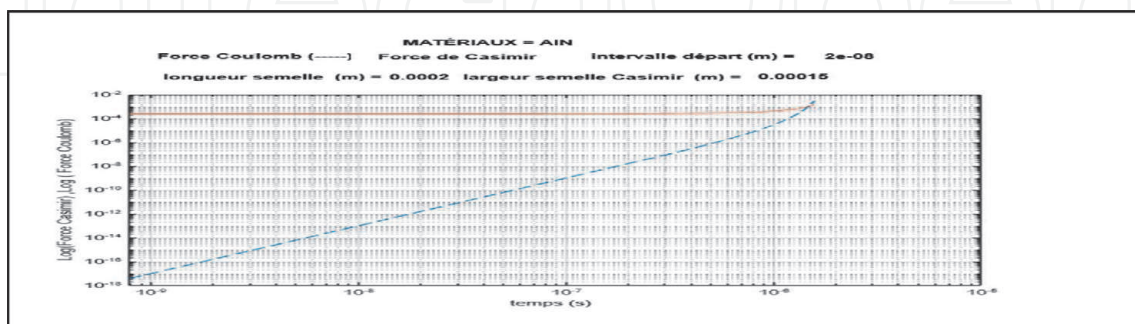*Piezoelectric Material = AlN Casimir, Coulomb Force = f (Time) starts Interface = 200 A °.*

This vibration frequency of the Casimir structure approaches that of the first resonance for weaker interfaces and less than 200 A°. We are then unfortunately confronted with the technological possibility of mastering such a weak interface.

It seems that the piezoelectric material PMN-PT coupled with a conductor like aluminum is an interesting couple for our vacuum energy extraction structure!

4.2.2 Piezoelectric material = AlN

With the MATLAB simulation of the behavior of the structure for piezoelectric Aluminum Nitride (AlN), we obtain the evolution with the time of the Casimir and Coulomb forces as well as the F_{CO}/F_{CA} ratio of **Figures 40** and **41** below. For a ratio F_{CO}/F_{CA} of 10, the maximum current delivered by the vibrating structure, the threshold voltage of the MOS and the vibration frequency of the structure is respectively $1.85 \ 10^{-7}$ A, Vt = 3.7 V and 667,000 Hertz.
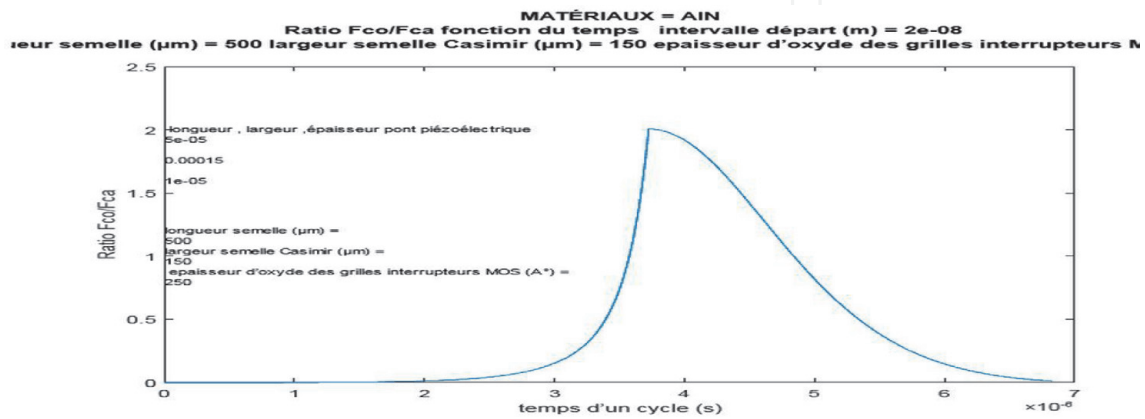
Figure 40.
Piezoelectric Material = AlN. Ratio F_{CO} / F_{CA} = f(Time). Start interface = 200 A °.
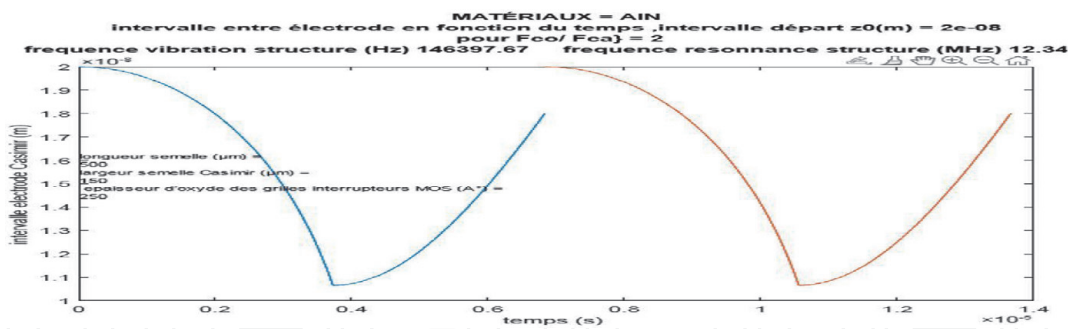
Figure 41.
Material = AlN Interval between Casimir electrodes = f (time) during two complete cycles: Interface between starting electrodes = 200 A °.
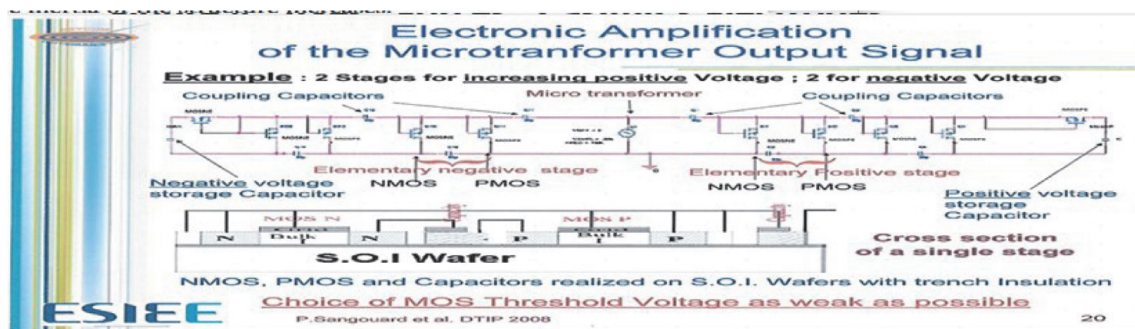

Figure 42.
Principle of electronics for amplifying and rectifying a week AC signal.

We observe (**Figure 42**) that the ratio p = F_{CO}/F_{CA} barely equals 2, and that the time of "rise" of the mobile Casimir electrode is relatively slow, it is a consequence of the low value of the piezoelectric coefficient d_{31} of AlN.

In conclusion, the use of AlN does not seem suitable for this vacuum energy extraction application.

4.3 Conclusions

It seems that for the piezoelectric material we used, the most suitable piezoelectric material for this vacuum energy extraction device is PMN-PT with a peak current of 350 m A, at least for the materials we used for the previous simulations (**Figures 7, 31–39**).

In order to convert these alternating current peaks into an alternating voltage without input of energy, this current passes through a L_{IN} inductor coil which converts these current peaks without input of external energy into voltage peaks of several volts and of a duration of the order of the nanosecond.

Inductors L_{IN} for printed circuits of the order of 100 μH or less are conventional and are commercially available.

The next chapter proposes to convert these peaks of alternating voltage, to amplify them to obtain a direct voltage of several volts without any external power supply!

5. Transformation and amplification electronics without external supply of a periodic signal of a few millivolts in a continuous voltage of a few volts

Consider the diagram in **Figure 5** which shows the location and configuration of the electronic circuits for collecting the current generated during a small fraction of the period of hypothetically inductance-sustaining vibrations of the structure. The mobile charges Q_{mn} at the terminals of the electrode S_{S2} are variable over time since they vary cyclically from null to $Q_{mn}/2$. A part of these electrical charges, in the ratio of the input impedance between the inductor L_{IN} and that of the transformer electronics of this signal, generate during the short durations of their homogenization time, a peak of current which go inside this inductor and create between the two terminals of this solenoid, a voltage peak.

In **Figure 5**, the gray and red surfaces are stationary, the others are free to move. The green metallic connector connects face n°1 (Sp1) of the piezoelectric bridge to the return electrode. The red metallic connector connects face n°2 (Sp2) of the piezoelectric bridge to the MOS gates. For circuit n°1: The MOSEN and MOSEP sources in // are connected to the metallic electrode of face n°1 of the piezoelectric bridge. The MOSE drains are connected in parallel to the electronics without external power supply for transforming the AC signal, and to a terminal of the L_{IN} solenoid. The other terminal of the inductance L_{IN} is connected to the return electrode if circuit 2 is open or to ground via circuits n°2 if it is conductive.

When, the enriched MOSNE and MOSPE of circuit n°1, connect face 1 to the return electrode via the inductance L_{IN}, as already seen, during this period the circuit composed of MOSND and MOSPD of circuit n°2 is then blocked. This connection occurs when their gates have a voltage making one of them ON.

When circuit n°1 is blocked, circuit n°2 is conducting and connects the return electrode to ground, which eliminates the charges present on this electrode and then prevents any electrostatic attraction.

We will describe these electronics designed and successfully tested at ESIEE with SPICE when I was studying abandoned sensors. This electronic without external energy gave very encouraging SPICE simulation results and delivers in its output an exploitable direct voltage when it have in its input an alternating and small signals!

In these SPICE simulations, the micro transformer was assimilated to a voltage source delivering a power U * I limited to a few nW (voltages of a few mV and current much lower than the microampere).

Now retired and no longer having sufficient means of simulations, I am simply describing the results of the SPICE simulations obtained in 2008.

The principle used to amplify and transform a weak signal without power supply derives from that of the diode bridge rectifier of Graetz or the doubler of Schenkel and Marius Latour.

The crippling problem is that the diodes of these rectifiers are conductive only with a minimum voltage of around 0.6 V at their terminals. As the alternating signal from the vacuum energy extraction device can be weaker, it is necessary to have switches that are triggered with a lower control voltage.

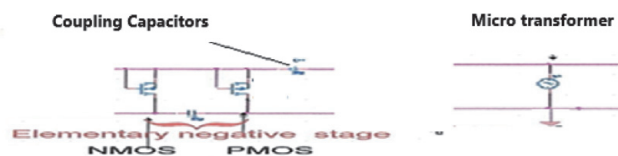The principal diagram of this electronics is presented in **Figures 43–45**.

Figure 43.
Elementary stage for obtaining a negative voltage from the alternative signal of the transformer (inductance). Start interface = 200 A °.
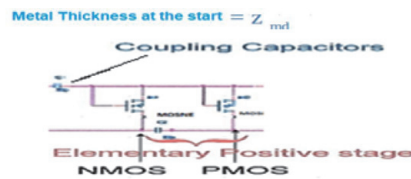

Figure 44.
Elementary stage for obtaining a positive voltage from of the alternative signal of the transformer (inductance) Start interface = 200 A °.
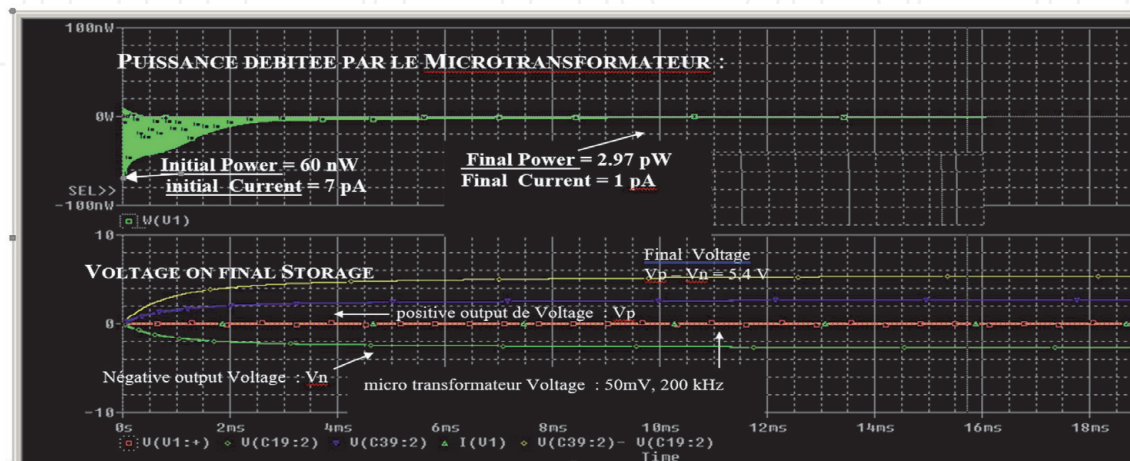

Figure 45.
SPICE simulations of voltages, current, power of the transformation electronics into a direct voltage (5.4 V) of an alternating input signal of 50 mV, frequency= 150 kHz, number of stage =14, coupling capacities = 20 pF, stocking capacity = 10 nF.

The MOSE N and P transistors of this rectifier circuit must have a technologically defined threshold voltage as close as possible to zero. The precision of nullity of these threshold voltages will depend on the values of alternating voltages at the terminals of the inductor L_{IN}, therefore on the second derivative of the temporal variations of the charges appearing on S_{p2} during the time of their homogenization which is of the order of: $t_e = R_m.C_s.Log$ (2) In the circuit of **Figure 8**, a micro transformer replaced the inductance L_{IN}. But this inductance plays the same role as this micro transformer since it delivers a limited power U.I.

The left part of the micro-transformer takes care of the negative voltages of the input signal, while the right part takes care of the positive voltages. The circuit is composed of several stages without no power supply which rectify and amplify, on the one hand the negative parts of the weak input signal and on the other hand the positive parts.

The number of elementary stages depends on the desired DC voltage, but this Dc voltage saturates with the number of stages in series (**Figure 46**). The results obtained from SPICE simulation are shown in **Figure 8**.

We observe an important point in **Figures 8** and **47**, the very low power and current consumption on the source since:

1. In **Figure 48** the power delivered by the source begin at the start with 60 nW and ends at 2.97 pW for an input current starting at 7 pA and finishing at 1pA.
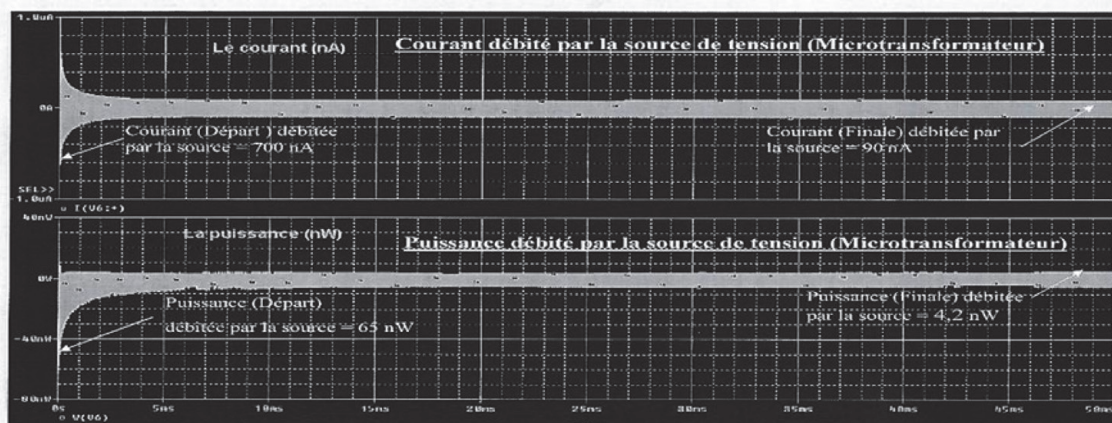

Figure 46.
SPICE simulations of the currents drawn by the transformer and the power consumed by this transformer. Input signal = 100 mV, frequency = 150kHz, number of stage = 30, coupling capacities = 20 pF, stocking capacity = 10 nF.
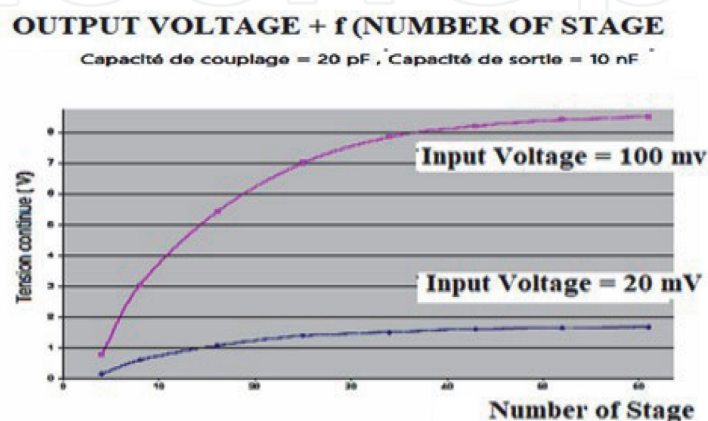

Figure 47.
DC output voltages as a function of the number of elementary stages for AC input voltages of 20 mV and the other of 100 mV. Start interface = 200 A °.

Output voltage = f(coupling capacitance), Nb of stages = 2*4 Storage
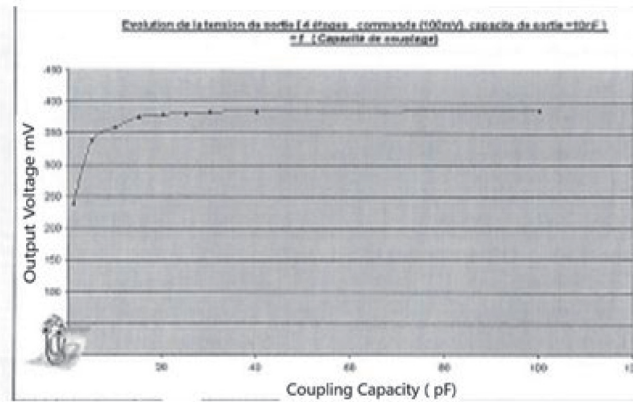capacitance = 10nF . Microtransformer input voltage =100mV

Figure 48.
Influence of the coupling capacitance on the amplification of the input signal. Start interface = 200 A °.

The negative component of the alternating signal is transformed in 10 ns into a negative direct voltage of $V_n = $ -2.7 V. Likewise the positive component the positive alternating part is transformed into a positive direct voltage of $V_p = $ 2.7 V We obtain therefore a direct voltage Vp-Vn = Vt = 5.4 V.

2. In **Figure 47** the power delivered by the source begin at the start with 65 nW and ends at 4.2 nW for an input current starting at 700 nA and finishing at 90 nA. The negative component of the alternating signal is transformed in 10 ns into a negative direct voltage of $V_n = $ -3.9 V. Likewise the positive component the positive alternating part is transformed into a positive direct voltage of $V_p = $ 3.9V. We obtain therefore a direct voltage Vp-Vn = Vt = 7.8 V.

An important point is the need to have a high circuit output impedance of several 10^7 ohms, so typically the input impedance of an operational amplifier.

The DC voltage obtained depends on the number of stages constituting these electronics without electrical power for transforming an AC signal of a few milli-volts into a DC signal of a few volts. However, this transformation saturates with the number of floors, as shown in **Figure 49** Note in **Figure 49** that the DC output
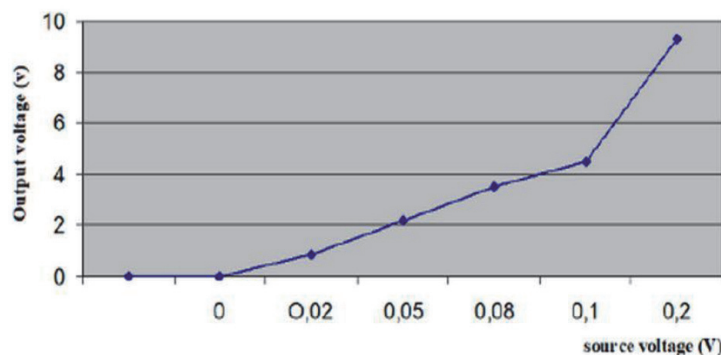
Figure 49.
Evolution of the DC output voltage as a function of the amplitude of the AC input signal for a frequency of 150 kHz. Start interface = 200 Å °
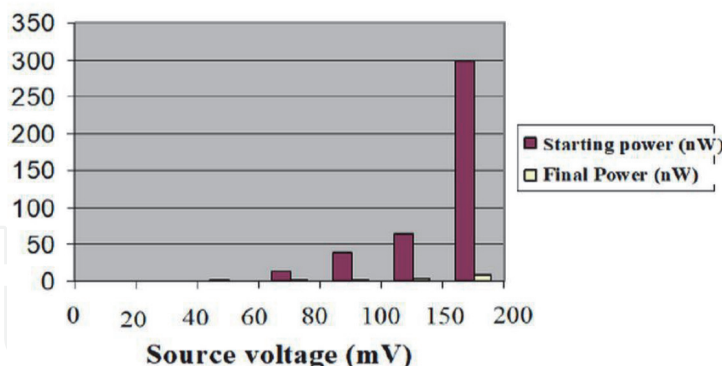
Figure 50.
Evolution of the power supplied in nW by the source as a function of the amplitude of the voltage supplied in mV. with 2 * 14 stages and a frequency of 150 kHz Start interface = 200 A °.

voltage saturates with the number of elementary stages and that the optimal number of stages is of the order of 40. We also looked at the influence of the coupling capacitance on the amplification of an input signal of 100 mV with a storage capacity of 10 nF. This amplification saturates and a coupling capacity of 20 pF which seems to be optimal signal (**Figure 48**).

The following **Figure 50** shows the influence of the value of the input AC voltage, with a frequency of 150 kHz, on the DC voltage obtained at the output of a 2 * 14 stage device.

Figure 46 shows the power in nW delivered by the source at the start of the amplification and at the end of this amplification.

A summary of the performance of this low "voltage doubler" device is shown in **Figure 51** below.

The interesting points for the presented electronics' device are:

1. the low alternative input voltages required to obtain a continuous voltage of several volts at the output

CHARACTERISTICS OF OUTPUT VOLTAGES (V), POWERS (nW) CURRENTS (nA)
AS A FUNCTION OF THE NUMBER OF STAGES
INPUT SIGNAL FREQUENCY = 150 kHz OUTPUT VOLTAGE MEASUREMENT FOR t = 50 ms

| number of stages | Vg=50mV | | | | | Vg=100mV | | | | |
| | Output Voltage | Current (nA) | | Power (nW) | | Output Voltage | Current (nA) | | Power (nW) | |
		start	end	start	end		start	end	start	end
2 *3	550mV	300nA	26nA	15nW	1.3nW	1.1v	800nA	46nA	75nW	5nW
2 *6	1	300nA	29nA	13nW	13nW	2V	700nA	67nA	60nW	6.5nW
2 *14	2.2v	300nA	40nA	14nW	2.6nW	4,5v	700nA	50nA	65nW	4.8nW
2 *21	2.8v	250nA	38nA	13nW	860pw	6v	600nA	80nA	60nW	2.7nW
2 *30	3.3	250nA	43nA	12nW	12nW	6.5V	750nA	85nA	61nW	4nW
2 *39	3.5v	250nA	45nA	12nW	900pW	7.5V	750nA	95nA	64nW	3.5nW
2 *48	3.6v	250nA	46nA	12nW	1nW	7.6V	750nA	100nA	60nW	4.2nW
2 *60	3.8	270nA	47nA	12nW	11nW	7.9V	700nA	90nA	65nW	4.2nW
2 *61	3.8	270nA	48nA	12.1nW	13nW	8 V	700nA	90nA	65 nW	42 nW

Figure 51.
Summary of transformations from low alternating voltages to direct voltage frequency of 150 kHz. Start interface = 200 A °.
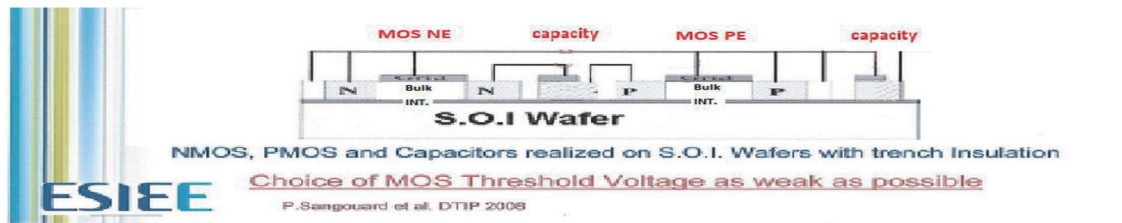
Figure 52.
S.O.I technology for making the elements of the "doubler".

2. the low power and current consumed by this conversion and amplification circuit on the source which in this case is only an inductor supplied by the current peaks generated by the autonomous vibrations.

3. the rapid time to reach the DC voltage (a few tens of milliseconds)

The technology used to fabricate the MOSNE and MOSPE transistors with the lowest possible threshold voltages is CMOS on intrinsic S.O.I. and the elements are isolated from each other on independent islands. This technology, represented in the following **Figure 52**, strongly limits the leakage currents.

We note that, the coupling capacities of 20 pF this electronic, like that of storage of the order of 10 nF, have relatively high values witch will require a square surface of:

- 120 μm^2 for a thickness of 250 A°, if the use silicon oxides SiO_2 with its relative permittivity of order of 4, which is a lot!

- Alumina Al_2O_3 obtained by oxidizing aluminum has only a relative permittivity of the order of 9 and would require alumina squares of 79 μm^2.

But if we use titanium dioxide as insulator, it has a relative permittivity of the order of 100 and is one of the most important for a metal oxide then the size of the capacity passes to 23 mm for a thickness of TiO2 = 500 A°, which is more reasonable!

6. Technology of realization of the current extractor device using the forces of Casimir in a vacuum

It can be seen in **Figures 25** and **26** that if PZT is used as the piezoelectric material, then the peak current output goes from 2.10^{-8} A to 6.10^{-8} A, when the width of the piezoelectric layer bp changes from 50 μm to 150 μm (for a length of the piezoelectric layer lp $= 50\,\mu m$, a thickness ap $= 10\,\mu m$, a length of the Casimir electrode ls $= 200\,\mu m$, starting interface $z_0 = 200$ A° and a Ratio of $F_{CO}/F_{CA} = 10$).

As a result, it will be necessary, using micro-technology techniques on S.O.I silicon, to machine devices with on a high thickness while maintaining exceedingly small spaces between structures Casimir. The microelectronics laboratory of the ESIEE has acquired a great experience in the plasma etching of deep sub-micron structures by etching remarkably parallel layers of silicon of 100 mm separated by intervals of 0.8 mm and well parallel [6, 7] and **Figure 53**.

However, for the structures presented above, the space between the two surfaces of the reflectors must be of the order of 200 A°, almost 4000 times less wide …. which is not technologically feasible by engraving!

Yet it seems possible, to be able to be obtained this parallel space of the order of 200 A° between Casimir reflectors, not by etching layers but by making them thermally grow!
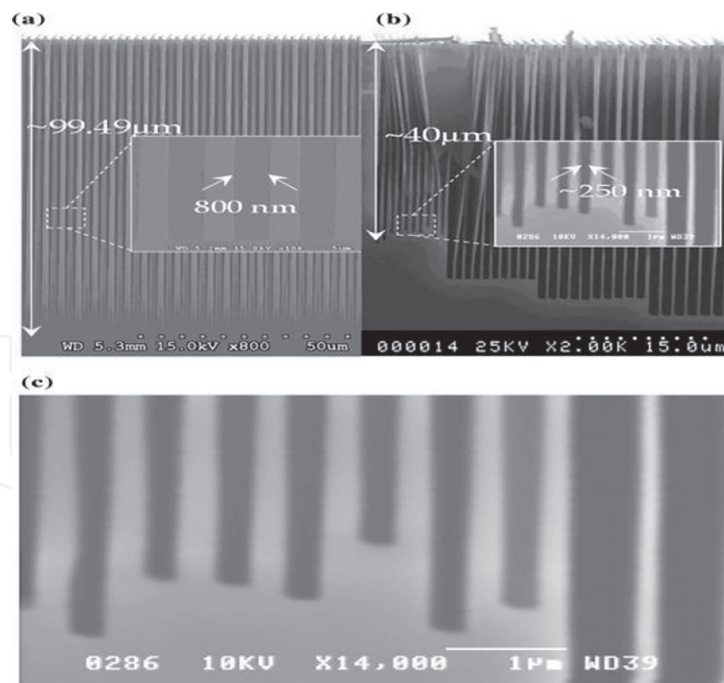
Figure 53.
Extract de [7]: High aspect ratio (HAR) structures manufactured using the Bosch process: (a) 800 nm-wide trenches with a depth of 99.5 lm (aspect ratio 124:1) and (b) 250 nm-wide trenches with a depth of 40 lm (aspect ratio 160:1). Some of the walls collapsed during the dicing procedure. © is a magnified view of the inset shown in (b) [8].

Indeed, the S_{S3} and S_{S2} surfaces of the Casimir reflector must;

- be metallic to conduct the mobile charges

- insulating as stipulated by the expression of Casimir's law who established for surfaces without charges! This should be possible if we grow an insulator on the z direction of the structure, for example Al_2O_3 or TiO_2 or other oxide metal which is previously deposited and in considering the differences in molar mass between the oxides and the original materials (see **Figure 33**).

For example, silicon has a molar mass of 28 g/mol and silicon dioxide SiO_2 has a molar mass of 60 g/mol. However, it is well known that when we grow a silicon dioxide SiO_2 of one unit we "attack" a silicon depth of the order of 28/60 = 46.6% (**Figure 54**).

The initial silicon layer reacts with the oxidizing element to form SiO_2. We will thus "consume" Silicon. The Si/SiO_2 interface will therefore end up "below" the initial surface. A simple calculation shows that the fraction of oxide thickness
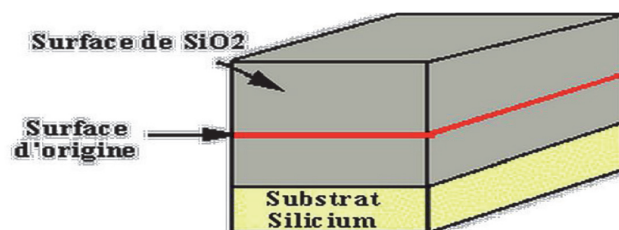

Figure 54.
Growth of SiO2 oxide on silicon.

"below" the initial surface is 46% of the total oxide thickness; the fraction "above" therefore represents 54% according to S.M. Sze. We therefore moved the original silicon surface by 46% [9].

The same must happen, for example for thermal growth of alumina. As the molecular masses of Alumina and aluminum are M_{Al2O3} = 102 g/mole and M_{Al} = 27 g/mole, we obtain an aluminum attack ratio of 27/102 = 26%, which implies that the original surface of this metal has shifted by 26% so that 74% of the alumina has grown out of the initial surface of the aluminum …. .

Likewise, if titanium is used for thermal growth of TiO_2, the molar mass ratio being M_{TiO2} = 79.9 g/mole and M_{Ti} = 47.8 g/mole we obtain a titanium attack ratio of 59.8% which implies that the original surface has moved by 59.8%.

So, this growth covers up the initial interface and it can be finely controlled! As a result, it should be possible to define finely the interface between the two Casimir reflectors using the oxidative growth conditions of a metal such as titanium or aluminum.

As regards the technological manufacture of electronics and structure, it therefore seems preferable:

1. For electronics to choose Titanium Oxide because of its high relative permittivity ε_r = 114 allowing to minimize the geometries required for the different capacities

2. For the Casimir structure, the choice of aluminum seems preferable, because its low density increases the resonant frequency of the structure and that 74% of the Alumina is outside the metal, allowing to reduce the interface between Casimir electrodes and that of the return electrode by Al_2O_3 alumina growth. A quite simple calculation shows for example that for aluminum (**Figure 55**):

We obtain: $z_{od} = 2^*(z_{md} + z_{of} - z_{ma}) + z_0 = 2^*(z_{md} + z_{of}(1 - .26)) + z_0$.

For example, if we start from an opening $z_{od} = 3\,\mu m$ and deposit a metal layer of aluminum that is etched leaving a width $z_{md} = 1\mu m$ on each side of the reflector. Then an Alumina Al_2O_3 can grow, the thickness of which is precisely adjusted, simply by considerations of time, temperature, and pressure to increase a necessary thickness to have a desired interface z_0.!

For example, if $z_0 = 200A°$, $z_{od} = 3\mu m$, $z_{md} = 1\mu m$, then $z_{of} = 0.662\mu m$. So, we obtain a Casimir interface of 200 A°. The final remaining metal thickness will be $z_{mf} = 0.338\,\mu m$ and will act as a conductor under the aluminum oxide.

Obviously, the growth of this metal oxide between the electrodes of the Casimir reflector modifies the composition of the dielectric present between these electrodes, therefore of the mean relative permittivity of the dielectric.

Let: ε_0 be the permittivity of vacuum and $\varepsilon_0 . \varepsilon_r$ the metal oxides one (ε_r = relative permittivity = 8 in the case of Al_2O_3), z_{of} the final oxide thickness on one of
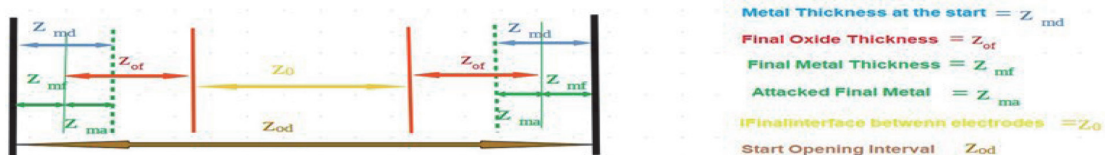

Figure 55.
Distribution of thickness.

the electrodes and z the thickness of the vacuum present between electrode (initially we want $z = z_0$).

Then the average permittivity e_{0m} of the dielectric is:

$$\varepsilon_{0\ m} = (z_{of}.\varepsilon_0 \cdot \varepsilon_r + z \cdot \varepsilon_0 + z_{of} \cdot \varepsilon_0 \cdot \varepsilon_r)/(2z_{of} + z)\varepsilon_{0m}$$
$$= \varepsilon_0 \cdot (2 \cdot z_{of} \cdot \varepsilon_r + z)/(2.z_{of} + z) \cong \varepsilon_0 \cdot \varepsilon_r$$

because z is $< < z_{of}$.!! For example, $z_{of} = 6620$ A° is large compared to $z < = 200$A° therefore $\varepsilon_{0m} \cong 8^*\varepsilon_0$ in the case of Al_2O_3.

We have taken this change in permittivity into account in the preceding simulations.

7. Steps for the realization of the structure and its electronics

We start by the voltage "doubler". These electronics are produced using CMOS technology with 8 ion implantations on an S.O.I wafer with an intrinsic silicon layer above the oxide:

1. To make the drains, sources of the MOSNE, MOSND of the "doubler" circuits, of the MOSNE and MOSND of the Coulomb force trigger circuit and of the grounding switches of the S_{S3} electrode of the Casimir reflector

2. To make the source drains of the MOSPE, MOSPD of the "doubler" circuits, of the MOSPEs and MOSPDs of the Coulomb force trigger circuit and the grounding switches of the S_{S3} electrode of the Casimir reflector

3. To best adjust the zero-threshold voltage of the MOSNE of the "doubler" circuit

4. To best adjust the zero-threshold voltage of the MOSPE of the "doubler" circuit

5. To define the threshold voltage of the MOSNE of the parallel circuit triggering the Coulomb force

6. To define the threshold voltage of the MOSPE of the parallel circuit triggering the Coulomb force

7. To define the threshold voltage of the MOSND of the series circuit for grounding the S_{S3} electrode of the Casimir reflector

8. to define the MOSPD threshold voltage of the series circuit for grounding the S_{S3} electrode of the Casimir reflector.

   Once this electronics is done, we are interested in the realization of the structure of CASIMIR with the following technology proposal:

9. engrave the S.O.I. silicon to the oxide to define the location of the Casimir structures (**Figure 56**)
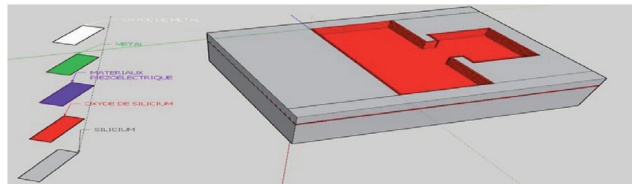
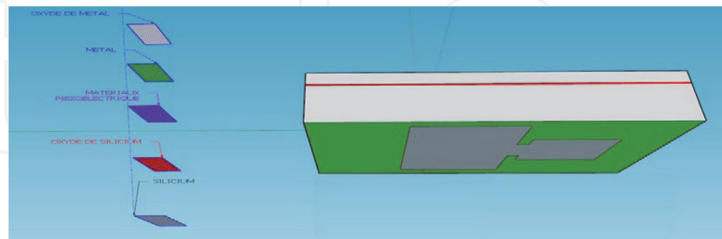**Figure 56.**
Etching of S.O.I silicon.

Figure 57.
Engraving of the protective metal rear face of the S.O.I. silicon.

10. Place and engrave a protective metal film on the rear faces of the S.O.I wafer (**Figure 57**)

11. Deposit and engrave the piezoelectric layer (**Figure 58**)

12. Depose and etch the metal layer of aluminum (**Figure 59**).

13. Plasma etching on the rear side the silicon of the Bulk and the oxide of the S. O.I wafer protected by the metal film to free the Casimir structure then very finely clean both sides (**Figure 60**)

14. Place the structure in a hermetic integrated circuit support box and carry out all the bonding necessary for the structure to function.
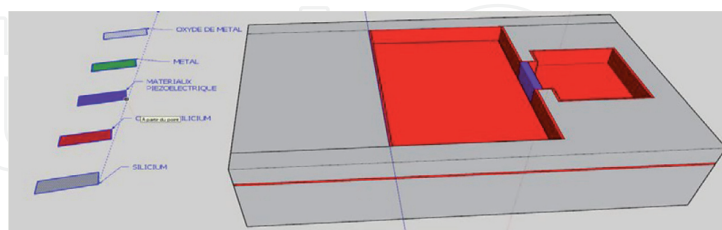
Figure 58.
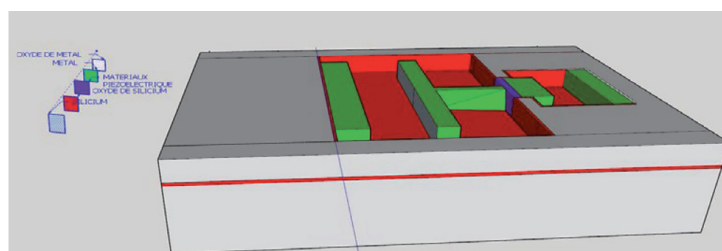*Deposition and etching of the piezoelectric layer e 61 deposition and etching of the piezoelectric layer.*

Figure 59.
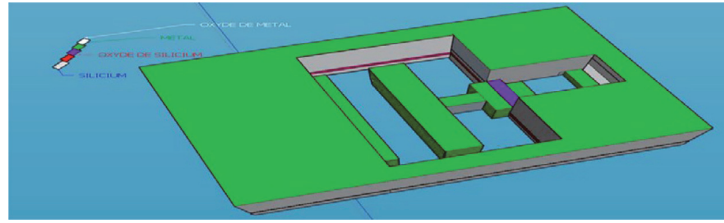*Metal deposit, metal engraving etching of the piezoelectric layer.*

Figure 60.
View of the Casimir device on the rear face, engraving on the rear face of the structures.
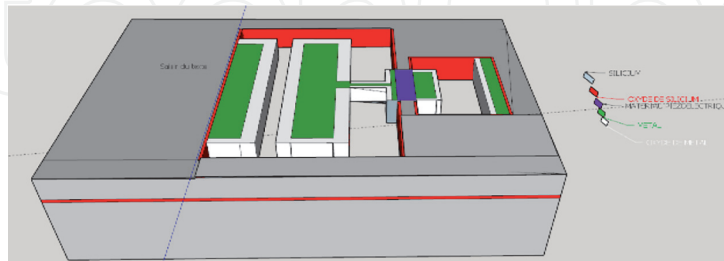

Figure 61.
Adjusted growth of metal oxide under the electronic control, front view of the Casimir device.

15. Carry out the thermal growth of aluminum oxide Al_2O_3 with *a measurement and control of the circuit under a box which should generate a signal when the interface between the Casimir electrodes becomes weak enough for the device to vibrate … and then stop the oxidation* (**Figure 61**).

16. Create a vacuum in the hermetic box

In the case where the 2 metal electrodes of Casimir which are separated by a very weak interface, of the order of 200 A°, adhere to one another, then these two surfaces can be separated by the application of an electrical voltage on the electrodes on the other side of the piezoelectric bridge!

In order to obtain a current peak greater in intensity and duration, the Casimir cells can be positioned in a series and parallel network at the 2 terminals of a single inductance. For example, 20 Casimir cells can be placed in parallel and 10 in series.
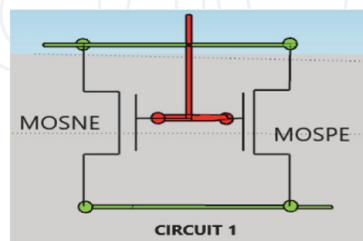
Circuit 1: parallel MOSPE and MOSNE ; see **Fig. 6**.
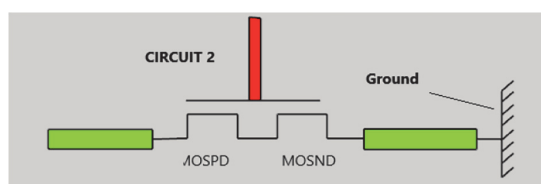
Circuit 2: serial MOSPD and MOSND ; see **Fig. 6**.

8. Energy balance

1. We remark that there is no bending of the free Casimir reflector electrodes. This only moving parallelepiped metallic electrode is in parallel to a fixed metal electrode defined on an S.O.I wafer and stay parallel to it. It transmits its motion to a piezoelectric bridge that deforms by bending.!

2. So the entropy expulsion ΔS from this Casimir vibrating structure and transmitted to the piezoelectric bridge is done by heat expulsion out of this bridge, but causes an extremely low temperature increase of the piezoelectric bridge!

A quick order of magnitude calculation gives: ΔQ_{vib} = heat transmitted by the vibrations of the piezoelectric bridge and evacuated outside follow, in first approximation, the well-known formula $\Delta Q_{vib} = \Delta S \Delta T \Delta Q_{vib} = \Delta S \, \Delta T$, with ΔS entropy variation ($J°K^{-1}$) and ΔT = temperature variation (°K).

However, we know that: (cf: M. BARTHES, M. Colas des Francs SOLID MECHANICAL VIBRATIONAL PHYSICS, ESTP: (Special School of Public Works).

$\Delta Q_{vib} = 1/2 * m(2\pi f_{vib})^2 x_{max^2}$; with: f_{vib} = Vibration frequencies of the piezoelectric bridge, m = mass of this bridge, x_{max} = maximum deflection of the bridge.

This heat, expended at the level of the piezoelectric bridge, causes a temperature increase.

As a first approximation we can say: $\Delta Q_{vib} = m C_{piezo} \Delta T$, with C_{piezo} = Specific heat capacity of the piezoelectric bridge ($J\,Kg^{-1}°K^{-1}$), $\Delta T = T$ emperature variation (°K).

Consequently $\Delta T = 2(\pi f_{vib})^2 x_{max^2}/C_{piezo}$ = Temperature variation.

We have for example:

$C_{piezo} = C_{PMN-PT} = 310 \left(J Kg^{-1°}K^{-1}\right), f_{vib} \cong 10^6 \, Hz, x_{max} \cong 100 * 10^{-10}$ m, we obtain: $\Delta T \cong 10^{-3°}K$ which is negligible!!

So, the expulsion of entropy from the vibrating Casimir Electrode is negligible! From 0 to z_e:

In a cycle from 0 to z, the energy $E_{Casimir}$ is: $E_{Casimir} = \int\limits_0^{ze} F_{ca} dz = \int\limits_0^{ze} \left(\frac{\pi^2 \hbar c}{240 z_S^4}\right) dz$.

No mobiles electric charges appear on the face of return electrode which is connected to the mass and isolated of the piezoelectric bridge, and so the Coulomb force disappears!

During this displacement "going" from 0 to ze the deformation of the piezoelectric bridge, generates a potential energy W_{Bridge} accumulated in the capacity of this bridge which follows the equation:

$$W_{Bridge} = \int\limits_0^{Q_e} \frac{Q_F}{Cpi} dQ_F = \left[\frac{Q^2_F}{2^* \, Cpi}\right]_0^{Q_e} = \frac{a_p}{2 \, l_p \, b_p \varepsilon_0 \varepsilon_{pi}}.$$

$$\left(\frac{d31 \, lp}{2ap}\right)^2 F^2_{CA} = \frac{a_p}{2 l_p \, b_p \varepsilon_0 \varepsilon_{pi}} * \left(\frac{d_{31} \, lp \, l_S b_S \pi^2 \hbar c}{480.ap}\right)^2 \left(\frac{1}{z_e}\right)^8$$

With Q_F the naturally creating fixed charges on this piezoelectric structure. $Q_F = \frac{d_{31} F_{CA} l_P}{a^P}$ Eq. (3),

$Q_e = -Q_F$ the accumulated mobile charges on both the two surfaces of the "return" electrode when coulomb's force triggered at $F_{CO} = p \, F_{CA}$, C_{pi} = electrical capacity of the piezoelectric bridge, z_e the position of appearance of the Coulomb force.

From z_e to 0:

For this very quick "returning" from position z_e to position 0, the associated energy $E_{Returning}$ is:

$$E_{Returning} = \int\limits_{ze}^{0} (F_{co} + F_{ca})dz = E_{Coulomb} - E_{Casimir}$$

Thus, we see that in the balance $E_{Casimir} + E_{Returning}, = E_{Coulomb}$. So, over a complete cycle, the energy $E_{Casimir}$ is conservative.!

The Coulomb energy $E_{coulomb}$ is the net energy appearing during a cycle. It is not due to any electrical energy applied, but to the consequence of vacuum energy!

If we choose $z_r = z_0$, the expression of $E_{coulomb}$ is,

$$E_{coulomb} = \left(l_S b_S \frac{\pi^2 \hbar c}{240} \frac{d_{31} l_P}{a_P} \right)^2 \left(\frac{1}{4\pi\varepsilon_0\varepsilon_r} \right) \int\limits_{ze}^{0} \left(\left(\frac{1}{z_s^4} - \frac{1}{z_0^4} \right) \right)^2 \left(\frac{1}{z_r + z_0 - z_S} \right)^2 dz$$

A Coulomb force then appears between these two electrodes.

$$F_{CO} = \left(S_S \frac{\pi^2 \hbar c}{240} \frac{d_{31} l_P}{2^* a_P} \left(\frac{1}{z_s^4} - \frac{1}{z_0^4} \right) \right)^2 \left(\frac{1}{4\pi\varepsilon_0\varepsilon_r} \right) \left(\frac{1}{z_r + z_0 - z_S} \right)^2 \right)$$

The position z_e of appearance of this force is such that $F_{CO} = p\, F_{CA}$, so if we choose $z_r = z_0$.

Then, the z_s position of appearance of this force is when:

$$\left(l_S b_S \frac{\pi^2 \hbar c}{240} \frac{d_{31} l_P}{2^* a_P} \left(\frac{1}{z_s^4} - \frac{1}{z_0^4} \right) \right)^2 \left(\frac{1}{4\pi\varepsilon_0\varepsilon_r} \right) \left(\frac{1}{2z_0 - z_S} \right)^2 = p l_S b_S \left(\frac{\pi^2 \hbar c}{240} \right) \frac{1}{z_s^4}$$

This position and evolution z_s are illustrated in the following **Figures 62** and **63**. As a result, the movement of the movable electrode shown in **Figure 62**.
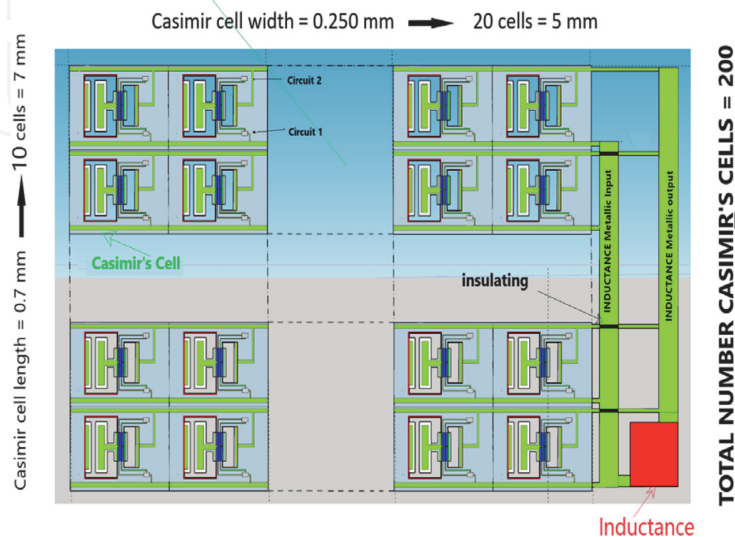

Figure 62.
Positioning of 20 Casimir cells in parallel and 10 in series. Circuit 1, Circuit 2 and Switches of circuit n ° 1 and n ° 2. Total of Casimir cells delivering a periodic current during a small part of the vibration frequency of the devices = 200!. Total des cellules = 200, width = 5 mm, length = 7 mm.
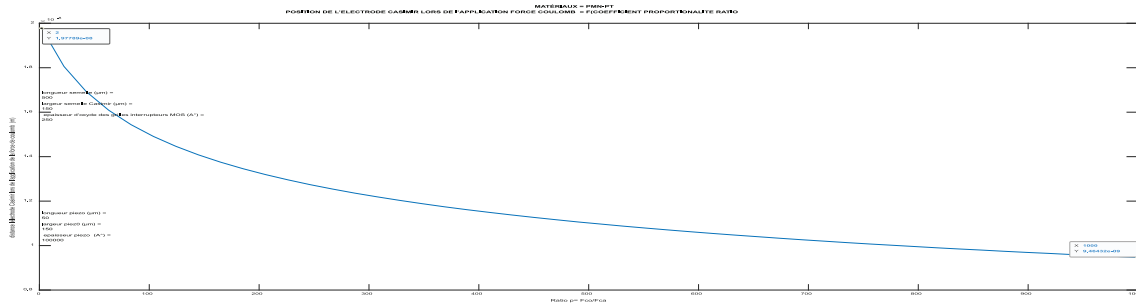
Figure 63.
Position of the mobile casimir electrode when the coulomb force occurs ls = 500 μm; bs = 150 μm; lp = 50 μm; bp = 150 μm; ap = 10 μm.

Note that the displacement of this mobile Casimir electrode is extremely small since it goes from 2 A° for an F_{CO}/F_{CA} ratio = 2 to 105 A° for a ratio of 1000.

When the electrical potential on the gate of the switches is greater than their threshold voltage, then this switch commute and the accumulated energy in the piezo electric's bridge will be used for the homogenization of the mobile charges of the bridge's electrodes connected to sources or drains of the MOS switch n°1 and the Coulomb return electrode.

During the time of this homogenization appears a current peak for a short time. So, an electrical voltage at the terminals of the self in series between switch 1 and the return electrode appears also!

So, an important point of obtaining current peaks related to the homogenization of charges appears.

His expression is: $I_{IN} = -\frac{Q_{mn2}}{R_m C_s}\left(Exp\left(-\frac{t}{R_m C_s}\right)\right)$.

With defining $t_c = R_m * C_s * ln\,(2)$ the duration with which the mobile charges equalize.

between the electrode of face 1 and the return electrode and R_m = the resistance (Ω) of the devices in series (Self + switch n°1); C_s the capacity (F) of the device constructed on face n°2 of piezoelectric bridge, return electrode).

These cyclic current peaks induce at the terminals of the coil voltage peaks whose expression is:

$$U_{IN} = L_{IN}\frac{d(I_{IN})}{dt} = L_{IN}\frac{Q_{mn2}}{R_m C_s}\left(Exp\left(-\frac{t}{R_m C_s}\right)\right) = L_{IN}\frac{Q_{mn2}}{R_m C_s}\frac{ln\,(2)}{t_e}\left(Exp\left(-\frac{t\,ln\,(2)}{t_e}\right)\right)$$

With L_{IN} the value of the inductance, Q_{mn2} the charges on the return electrode and the face n°1 of the bridge.

The only energy which is effectively used outside, during one cycle, is associated with these current and voltage peaks becomes:

$$W_{electic} = Abs\left(\int_0^{t_e}\frac{I_{IN}\,UIN}{2}d(t)\right) = \frac{L_{IN}}{2}\left(\frac{d_{31}F_{CA}l_P}{a_P}\right)^2\left(\frac{ln\,(2)}{te}\right)^2(1 - Exp(-2\,ln\,(2)))$$

$$(20)$$

For example, we obtain, for an interface between Casimir's electrodes $z_0 = 200$ A°, dimensions of the Casimir electrodes (length = 500 μm, width = 15 μm, thickness = 10 μm), dimensions of the piezoelectric bridge in PMN-PT (length = 50 μm, width = 15 μm, thickness = 10 μm), a proportionality factor p = F_{CO}/F_{CA} = 1000, an inductance $L_{IN} = 1.10^{-6}$H:

- $Z_e = 9.46 \, 10^{-09}$ (m) i.e., a displacement of the mobile Casimir electrode of about 105A° (**Figure 63**)

- $W_{CA} = E_{Casimir} = 3.4 \, 10^{-11}$ (Joule) = Energy of vacuum = Energy dispensed by the force of Casimir

- $W_{bridge} = 2.7 \, 10^{-11}$ the potential energy accumulated in the piezoelectric bridge

- Peak current = $350 \, 10^{-6}$A

- Voltage peak across the coil = 1.2 V

- Structure vibration frequency = 750 kHz

- Threshold Voltage of enriched MOSE = Threshold Voltage of in depletion MOSD = 3.25 V

- $W_{electric} = 2.7 \, 10^{-11}$ (Joule) = Usable energy associated with current and voltage peaks.

We remark that this energy $W_{electric}$ is equal to the energy W_{bridge} accumulated in the bridge and is not brought by an external electrical source but is caused by the omnipresent and perpetual force of Casimir, itself controlled by a Coulomb force of opposite direction.

This Energy is less than that developed by Casimir's strength.

- The intensity of the Coulomb force is defined and technologically adjustable by adjusting the threshold voltage of the MOS transistors of circuits 1,2,3,4.

- ΔQ_{vib} = heat transmitted by the vibrations of the piezoelectric bridge = $7.8 \, 10^{-14}$ J and is very small.

- We notice that $\Delta Q_{vib} + W_{electric} < E_{Casimir}$ which is consistent with Noether's theorem.

This energy $W_{electric}$ is equal to the energy W_{bridge} accumulated in the bridge and not brought by an external electrical source, but is caused by the omnipresent, timeless and perpetual force of Casimir, itself controlled by a Coulomb force of opposite direction.

Remember that Energy is defined as the "physical quantity that is conserved during any transformation of an isolated system." However, the system constituted by simply the MEMS device is not an isolated system.

On the other hand, the system constituted by the MEMS device plus the vacuum becomes an isolated system.

A system of 200 structures (**Figure 64**) gives a usable energy by second and so 750,000 peaks, $W_{electric} \cong 60 \, 10^{-3}$ (Joule) for a coefficient of proportionality $p = F_{CO}/F_{CA} = 10^6$ and all switch transistors (Width = Length = 100 μm, SiO$_2$ grid thickness = 250 A°), thresholds voltage = 3 V.

This energy is not brought by an external electrical source but is caused by the omnipresent and perpetual force of Casimir, itself controlled by a Coulomb force of opposite direction.

This Coulomb force appears by the automatic switching of MOS transistors when its intensity is greater than a predetermined value and opposite to that of the Casimir force.
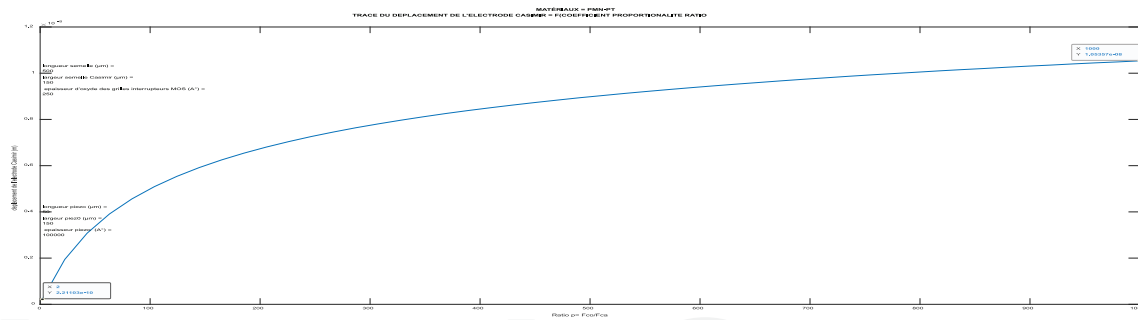
Figure 64.
Displacement of the mobile casimir electrode during the appearance of the coulomb force ls = 500 μm, bs = 150 μm, lp = 50 μm, bp = 150 μm, ap = 10 μm.

This technologically programmable switching of the MOS switches induces the spontaneous appearance of current peaks during a few nanoseconds, themselves inducing voltage peaks at the terminals of an inductor. When the system returns to its starting position, the Coulomb force disappears, leaving the Casimir force to deform the structure again.

The system then spontaneously enters into vibrations.

The energy balance of a cycle therefore seems to satisfy Emmy NOTHER's theorem!

9. Conclusions

1. the proposal to use isotropic and perpetual energy of Casimir called Energy of the vacuum, to obtain a variation of electric charges of a piezoelectric bridge which generates current peaks at the frequency of inductance-sustaining vibrations of the structure, usable without no energy input

2. the system which should allow the conversion of this vacuum energy into alternating current peaks at the vibration frequency of the system. This current passes through an inductor which converts these alternating current peaks into alternating voltage peaks.

3. The current and the voltage at the terminals of this choke feed electronics which rectifies and amplifies, without any external power supply, these voltage peaks in a direct voltage of a few usable volts.

4. a proposal for micro and nano electronic technology giving hope for a possible realization of this set.

According to this study, it would seem we can extract energy from the vacuum by the use of the Casimir force thwarted at the appropriate time by a temporary Coulomb force which makes the system return to its initial position and makes enter into vibrations the structure!!

I am fully aware that this concept may sound like incredible, but it does not seem to contradict Emmy Noether's theorem and, mathematical calculations and simulations give encouraging results and merit further study of this concept by a thesis. I am looking for a microelectronics laboratory with sufficient technological and design resources to confirm or deny this idea of a retired dreamer. The dreamer would be happy to participate in this dream of a new source of energy.

A. Appendices

A.1 A few reminders from RDM

A.1.1 Calculation of the deflection of a bridge embedded at its 2 ends

Note: We take the case of pure bending, the shear force T is such that With M the bending moment applied to the piezoelectric bridge. The Casimir force in the z axis is applied in lp/2 at the center of the bridge (**Figure 65**).

Recall that the neutral axis G (x), is the place where the normal bending stress is zero. G is a point of this neutral axis which in the case of a symmetrical bridge is also on the median line of the center of gravity of the bridge. Let us name:

- M_Z (x) = Bending moment depending on the position x on the bridge,

- Gz a point of the neutral axis, z = f (x) the deformation of the bridge

- $I_P(x)$ the bending moment of inertia of the bridge section

- Ep the Young's modulus of the piezoelectric material

- ρ = the radius of curvature of the deformation z = f (x) the deformation of this bridge.

We will assume that the strains of the bridge subjected to the weak Casimir force are themselves small, so the induced strain angles d (ρ) are also small. Thus as it is stipulated in all the works of R.D.M. we can assimilate the radius of curvature ρ with Eq. (21) (**Figure 66**)

$$\tan (d\omega) = \frac{dx}{\rho} \approx \omega \Rightarrow \frac{1}{\rho} = \frac{d\omega}{dx} = -\frac{M_Z(x)}{E_P I_P(x)}$$

Since the bridge is parallelepiped in shape, the bending moment of inertia along the z axis of the section of this bridge is Eq. (22) (**Figure 67**)
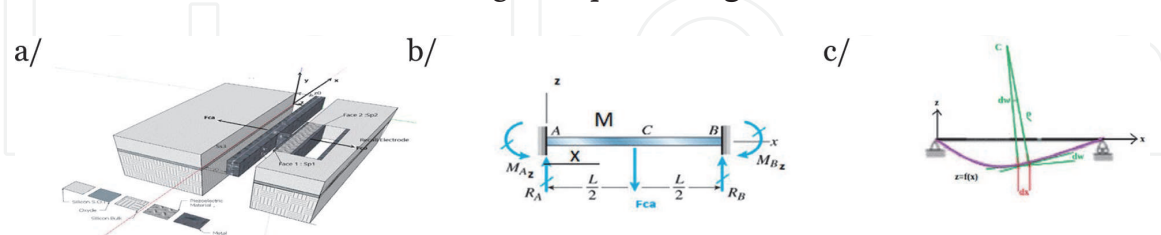
a/   b/   c/

Figure 65.
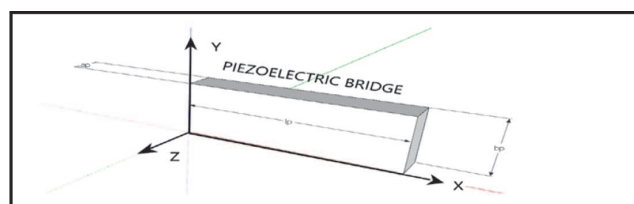*General appearance a/ b/ of the device studied, forces and applied moments, c/ of the deformed bridge.*

Figure 66.
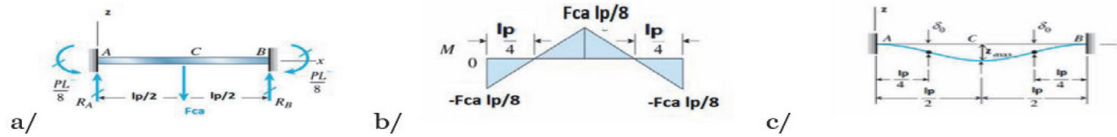*Piezoelectric Bridge Nomenclature.*

Figure 67.
(a) Forces, shear forces and moments applied on the bridge. (b) Variation of bending moment. (c) Shape and arrow of the bridge embedded at both ends. With: δo = inflection points, z_{max} = arrow of the bridge.

$$I_{GZ} = \frac{b_P a_P^3}{12} = Cte$$

$$In\, x = \frac{l_P}{2} \Rightarrow \frac{dz}{dx}_{x=\frac{lP}{2}} = 0 \Rightarrow MAZ(x = lp/2) = -\frac{F_{CA}}{8}lP \Rightarrow MAZx = 0) = -\frac{FCA}{8}lP$$

The maximum deflection is in x = lp/2 which gives an arrow: $z_{max} = F_{CA} \cdot l_P^3/(192\, E_P \cdot I_P)$ in $x = l_P/2$ (Eq. (23)). See RDM nomenclature

A.1.2 Calculation of the resonant frequency of the piezoelectric bridge

It is demonstrated (*see for example: Vibrations of continuous media Jean-Louis Guyader (Hermes)*) that the amplitude z (x, t) of the transverse displacement of a cross section of the beam is given by the partial differential equation: $\frac{\delta^4 z}{dx^4} + \frac{\rho S}{E_P IP} \frac{d^2 z}{dt^2} = 0$ if one neglects the internal damping!

The linear mass m(x) being equal to ρ_S (Kg/m), with ρ the density (Kg/m^3) and S the section (m^2), hence the differential equation of free vibrations deduced is: (Eq. (28)) $\frac{\delta^4 z}{dx^4} = -\frac{\rho S}{E_P IP} \frac{d^2 z}{dt^2}$ With $k = \left(\rho S \omega^2 / E_P I_P\right)^{1/4}$, the solution of this differential equation is.

written in the general form: $Z(x) = A1 \exp(k\, x) + A2 \exp(-k\, x) + A_3 \exp(i\, k\, x) + A_4 \exp(i\, k\, x)$ and in the more convenient form:

$$Z(x) = a \cdot \sin(k \cdot x) + b \cdot \cos(k \cdot x) + c \cdot sh(k \cdot x) + d \cdot ch(k \cdot x) \qquad (21)$$

A.1.2.1 Eigen modes and frequencies

In this part, we will assume that the moving part of the structure (**Figure 28**) vibrates at its resonant frequency. The only series of discrete pulsations w_i (proper pulsations of vibration) will be authorized, these pulsations being obtained in the general form: with: w_{pi} = resonance pulsation and therefore f_{pi} = frequency resonant

$$\omega_{PR} = \left(\frac{\alpha_I}{lP}\right)^2 \sqrt{\left(\frac{E_P IP}{\rho S}\right)} \Rightarrow f_{PI} = \frac{1}{2\pi}\left(\frac{\alpha_I}{lP}\right)^2 \sqrt{\left(\frac{E_P IP}{\rho S}\right)}$$

A.1.2.2 Boundary conditions

In our situation we have a recessed-recessed bridge. $Z(x) = a \cdot \sin(k \cdot x) + b \cdot \cos(k \cdot x) + c \cdot sh(k \cdot x) + d \cdot ch(k \cdot x)$ (30).

In this case for x = 0 and for x = lp, we have z(x) = 0 and dz./dx = 0 (zero elongations and slopes). Let:

For : x = 0 : 1 : a + c = 0a = −c2 : b + d = 0b = -d

For x = lp : 3 : a sin (k lp) + b cos (k lp) + c sh(k lp) + d ch(k lp) = 0;

4 : a cos (k lp)-b sin (k lp) + c ch(k lp) + d sh(k lp) = 0

We deduce from the preceding Eqs. (1–4) that: c. (sh (k lp) − sin (k lp)) + d (ch (k lp) − cos (k lp)) = 0; and c. (ch (k lp) − cos (k lp)) + d (sh (k lp) + sin (k lp)) = 0.

These last 2 equations lead to a transcendent equation in k l_p: so, the determinant of this system is

zero! $\left[\text{sh } (k.lp)^2 - \text{sin } (k.lp)^2\right] - [\text{ch } (k.lp) - \text{cos } (k.lp)]^2 = 0$ cos (k.lp) = 1/ch (k.lp).

The solutions of this equation can be solved graphically or numerically.

The numerical resolution (for example by the dichotomy method in **Figure 68** of this equation gives for the first 5 solutions: a1 = 4.7300; a2 = 7.8532; a3 = 10.9956; a4 = 14.1317; a5 = 17.2787.

So, the first resonant frequency of the piezoelectric bridge is.

$$\omega_{P1} = (4.73)^2 \sqrt{\frac{E_pI_p}{M_Sl_P^3}} \Rightarrow f_{P1} = \frac{1}{2\pi}(4.73)^2 \sqrt{\frac{E_pI_p}{M_Sl_P^3}} \text{ (31)}.$$

For example, for a bridge embedded at both ends with the following characteristics,

For geometries:

lp = 50 μm,bp = 150 μm,ap = 10 μm; Sp = 1,5$10^{-9}$ m^2,

Ip = bp · ap3/12 = 1.25$10^{-20}$ m^4

li = 10 μm; bi = 150 μm; ai = 10 μm; ls = 1000 μm; bs = 150 μm; as = 10 μm

For the material: PZT: density

$$r = 7600 \, (\text{kg/m}^3), \text{Young's modulus Ep} = 6^* \, 10^{10} \, (\text{Pa}) \, (\text{Kg m s}^{-2})$$

For the section inertia: Ip = bp* ap^3/12 = 1.25 10^{-20}(m^4).

Then the calculated first resonance frequency is for the PZT material: fp1 = 1.1553 * 10^7 hertz. For this embedded bridge, an ANSYS simulation (**Figure 69**) gives a resonant frequency of f1 = 1.02. 10^7 Hz which is close to that calculated in the draft calculation presented in this report and validates the orders of magnitude obtained with the equations for these preliminary calculations. If one carries out the calculation of the resonant frequency of the structure of **Figure 5** which comprises a free sole of Casimir S_{S2} parallel to a fixed surface S_{S3} and transmitting by a mechanical link finger the force of Casimir, one finds that the resonant frequency have the same form but with Ms. a fixed mass applied in the middle of the bridge. M_s = the total mass of the structure! $M_s = r(S_p{}^* a_p + S_i{}^* a_i + S_s{}^* a_s) = r(l_p{}^* b_p{}^* a_p + l_i{}^* bi^* a_i + l_s{}^* b_s{}^* a_s)$.
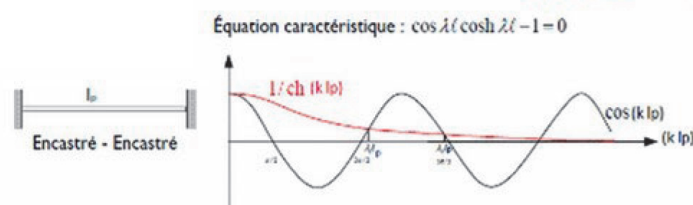

Figure 68.
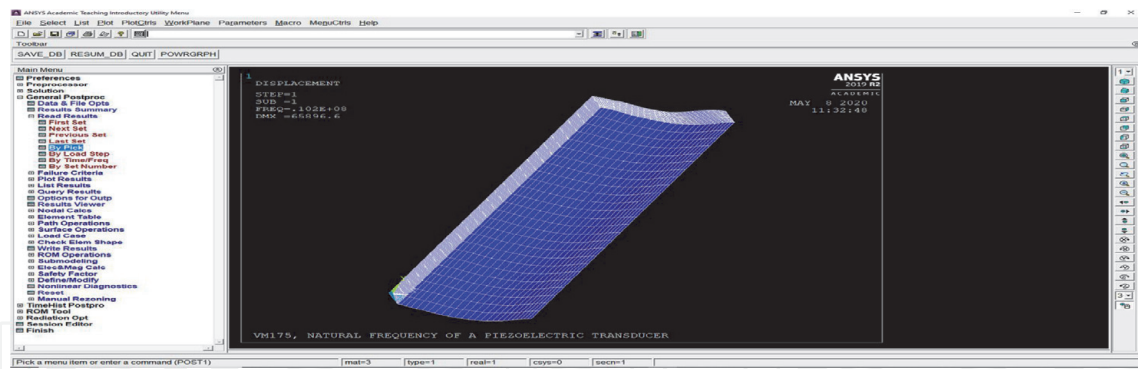*Numerical solution of Eq. (18).*

Figure 69.
ANSYS simulation of the resonant frequency of the piezoelectric.

With r = the medium density of the piezoelectric material, of the connecting finger, of the Casimir electrode sole and S_p,S_i,S_s the longitudinal surfaces of this bridge. Indeed, the presence of the Casimir sole connected by the Casimir force transmission finger in the middle of the piezoelectric bridge, modifies the resonant frequencies of this bridge.

The calculated resonance frequency then becomes for the same geometries and materials. fs1 = 2.509 10^6 hertz. With these characteristics, an ANSYS simulation of this structure gives a close resonance frequency: fs1 = 2.62 10^6 Hertz. This approach greatly simplifies these preliminary calculations because otherwise the curvature of the piezoelectric bridge makes the Casimir force strongly depend on the longitudinal and transverse positions x and z of the facing surfaces!

Author details

Patrick Sangouard
Mathematization, Simulation, Electronics, and Technology, Dijon, France

*Address all correspondence to: patrick.ps.patrick@gmail.com

IntechOpen

References

[1] Reynaud S, Lambrecht A, Jaekel MT. Fluctuations du vide quantique. In: Laboratoire Kastler Brossel UPMC case Jussieu F Paris Cedex 05. F 75231 Paris Cedex 05: Laboratoire de Physique Théorique de l'ENS 24 rue Lhomond; Juin 2001

[2] Casimir HBG. On the attraction between two perfectly conducting plates. Proceedings of the Koninklijke Nederlandse Akademie van Wetenschappen. 1948;**51**:793

[3] Deriagin BV, Abrikosova II. Direct measurement of the molecular attraction of solid bodies. 2. Method for measuring the gap. Results of Experiments. Soviet Physics JETP. 1957;**3**:819

[4] Lifshitz EM, Pitaevskii LP. Landau and Lifshitz course of theoretical physics: Statistical physics part 2 ch VIII (Butterworth-Heinemann, 1980). Soviet Physics JETP. 1956;**2**:73

[5] Techniques de l'Ingénieur 14/12/ 2012: l'expertise technique et scientifique de référence « Applications des éléments piézoélectriques en électronique de puissance » Dejan VASIC: Maître de conférences à l'université de Cergy-Pontoise, Chercheur au laboratoire SATIE ENS Cachan, François COSTA: Professeur à l'université de Paris Est Créteil, Chercheur au laboratoire SATIE ENS Cachan

[6] Wachel JC, Bates CL. Techniques for controlling piping vibration failures. ASME Paper. 76-Pet-18. 1976

[7] Parasuraman J, Summanwar A, Marty F, Basset P, Angelescu DE, Bourouina T. Deep reactive ion etching of sub-micrometer trenches with ultra-high aspect ratio. Microelectronic Engineering. 2014;**113**:35-39

[8] Marty F, Rousseau L, Saadanya B, Mercier B, Français O, Mitab Y, et al. Advanced etching of silicon based on deep reactive ion etching for silicon high aspect ratio microstructures and three-dimensional micro- and nanostructure. Microelectronics Journal. 2005;**36**: 673-677

[9] Semiconductor Devices, Physics' and Technology S. M. SZE Distinguished Chair Professor College of Electrical and Computer Engineering National Chiao University Hsinchu Taiwan, M.K. LEE Professor Department of Electrical Engineering, Kaohsiung Taiwan